



DELFT UNIVERSITY OF TECHNOLOGY

FACULTY OF MECHANICAL, MARITIME AND MATERIALS ENGINEERING

DEPARTMENT OF BIOMECHANICAL ENGINEERING

# NITINOL DRUG ELUTING SURFACES FOR CORONARY STENTS

---

<b>Student:</b>	Martina Cuschieri (4118995)
<b>Program of Study:</b>	M.Sc. BioMedical Engineering (BME)
<b>Specialization:</b>	BioMedical Materials (BMM) 2011/2012
<b>Supervisors:</b>	Dr. Ir. L.E. Fratila-Apachitei Prof. Dr. Ir. J. Duszczuk
<b>Date of Submission:</b>	22/10/2012





The research work disclosed in this publication is partially funded by the Strategic Educational Pathways Scholarship (Malta). This scholarship is part-financed by the European Union - European Social Fund (ESF) under Operational Programme II - Cohesion Policy 2007-2013, "Empowering People for More Jobs and a Better Quality of Life".



Operational Programme II - Cohesion Policy 2007-2013  
*Empowering People for More Jobs and a Better Quality of Life*

Scholarship part-financed by the European Union  
European Social Fund (ESF)  
Co-financing rate: 85% EU Funds; 15% National Funds



*Investing in your future*



Copyright © M. Cuschieri B.Eng.(Hons)(Melit.)  
All rights reserved.





## PREFACE

This report consists of two parts, namely: an article which summarizes the most important results obtained during my graduation project and a thesis which describes all the work done during this project. I hope you will enjoy reading it as much as I enjoyed working on this project (notwithstanding the difficulties encountered).

Martina Cuschieri



## ACKNOWLEDGEMENTS

I would like to express my most sincere gratitude to Dr. Lidy E. Fratila Apachitei for imparting her invaluable knowledge and advice and for her constant guidance, support and interest throughout this project.

Special thanks are directed to Mr. Maarten Gorseling and Mr. Michel van den Brink for their indispensable assistance during HPLC analysis.

I would also like to express my gratitude towards Dr. Zighuan Huan for his help with SEM imaging and for showing no hesitation in offering his advice and help whenever it was required.

I would like to take this opportunity to thank all my tutors during this two-year course whose tuition has directly or indirectly influenced this dissertation and for being inspirational role models. I would also like to thank Dr. Ing. John C. Betts, and Dr. Ing. Zdenka Sant for their continued interest during the last two years – thanks for your occasional emails and for the long chats we had whenever I came home.

Being so far away from home, we international students end up making brothers and sisters rather than making friends. I would therefore like to send a big hug to all of you who made these years in Delft so special. In particular, I would like to thank Magaly for being my Mexican shadow in the first year, to Ivo, Nishant, Ashwin and Paula for making lunch and coffee time the best time of the day during the second year, to Francesco for being the best desk-neighbour ever and for your contributions to lunches and coffee times, to Tassos for being the brother I never had (I will never forget that doner we had eaten together on the very first day) and to Vasilis, Renata, Tina, Joan, Dimitris, Kostas, Phaedra and all the rest for being part of my life – I love you all.

I would also like to extend my thanks to the Roelse's and the Tienhoven's for always being there for us and for making me feel part of the family. You gave us a home away from home.

I would like to thank my family and friends back in Malta for their constant patience, prayers, encouragement and support.

Last but not least I would like to thank Daniel, for being my neighbour and later also my room-mate, for not complaining too much about my mess and for always washing the dishes. Thanks for embarking on this journey together with me; thanks for all the times you comforted me and for the times you made me laugh. Thanks for listening to me when things didn't go too well and for trying to help me find solutions to my problems. Inñobbok hafna.

Tina



"The man who comes back through the door in the wall will never be quite the same as the man who went out. He will be wiser but less sure, happier but less self-satisfied, humbler in acknowledging his ignorance yet better equipped to understand the relationship of words to things, of systematic reasoning to the unfathomable mystery which it tries, forever vainly, to comprehend."

***Aldous Huxley***



# TABLE OF CONTENTS

<b>Part I: Scientific Article.....</b>	<b>vii</b>
<b>Part II: Thesis Report.....</b>	<b>ix</b>
<b>List of Figures .....</b>	<b>xi</b>
<b>List of Tables.....</b>	<b>xiii</b>
<b>List of Abbreviations .....</b>	<b>xiv</b>
<b>1 Introduction .....</b>	<b>1</b>
1.1 Background .....	1
1.2 Aim Of The Project.....	6
<b>2 Materials and Methods .....</b>	<b>7</b>
2.1 Material Used .....	7
2.2 Surface Treatment .....	7
2.2.1 Electropolishing .....	7
2.2.2 Plasma Electrolytic Oxidation .....	8
2.3 Surface Characterization.....	8
2.3.1 Scanning Electron Microscopy and Energy Dispersive Spectroscopy....	8
2.3.2 Surface Porosity Characterization .....	9
2.3.3 Surface Profilometry – Roughness Measurement.....	9
2.3.4 Drop Shape Analysis .....	10
2.4 Drug Loading and Release .....	11
2.4.1 Drug Loading.....	11
2.4.2 Drug Release .....	13
2.4.3 Drug Stability .....	14
2.4.4 High Performance Liquid Chromatography (HPLC) .....	15
2.5 Mathematical Modelling of Drug Elution .....	16

<b>3</b>	<b>Results and Discussion .....</b>	<b>19</b>
3.1	Surface Characterization .....	19
3.1.1	SEM and EDS Analysis .....	19
3.1.2	Surface Porosity Characterization.....	20
3.1.3	Roughness Measurement .....	21
3.1.4	Drop Shape Analysis.....	22
3.2	6-MP Loading and Release .....	23
3.2.1	6-MP Solubility .....	23
3.2.2	Effect of Spraying Conditions on 6-mp Loads and Surface Distribution 24	
3.2.3	Effect of PEO treatment on drug loading.....	31
3.2.4	<i>In Vitro</i> Release Profiles .....	33
3.2.5	Drug Stability.....	34
3.2.6	Effect of Modified Conditions on <i>In Vitro</i> Release .....	36
3.3	Mathematical Modelling of Drug Elution .....	38
<b>4</b>	<b>Conclusions .....</b>	<b>43</b>
<b>5</b>	<b>Suggestions for Future Work.....</b>	<b>44</b>
<b>6</b>	<b>List of References .....</b>	<b>47</b>





# **NITINOL DRUG ELUTING SURFACES FOR CORONARY STENTS**

---

## **PART I: SCIENTIFIC ARTICLE**



# Investigation of the Potential of Microporous TiO<sub>2</sub> Generated at the Surface of Nickel-Titanium by Plasma Electrolytic Oxidation to Act as a Polymer-Free Drug Delivery System

---

## Abstract

Nowadays, drug eluting stents (DES) are the treatment of choice for *de novo* atherosclerotic lesions. Novel DES are shifting to polymer-free (PF) drug delivery in order to avoid the problem of late stent thrombosis associated with long term polymer presence in the vessel lumen. The scope of this study was to assess the potential of a microporous layer of TiO<sub>2</sub> produced on Nitinol by means of electropolishing followed by plasma electrolytic oxidation (EP+PEO) to act as a PF carrier for 6-mercaptopurine, which is a novel anti-restenotic drug. The surface porosity obtained was characterised and the roughness and hydrophilicity of the samples were measured. The drug has been loaded by spray coating and its release in acidified Phosphate Buffered Saline over a period of 5 days was analysed by high performance liquid chromatography. The results obtained were compared to those obtained from electropolished samples loaded under similar conditions. The findings revealed that EP samples had a drug loading efficiency of 26.8%, a drug reservoir capacity of 18.2 µg/cm<sup>2</sup> and released 95% of the loaded drug within 10 minutes of immersion. On the other hand, EP+PEO samples, with a surface porosity of about 10%, showed a drug loading efficiency of 41.9%, a drug reservoir capacity of 30.6 µg/cm<sup>2</sup> and released 42% of the drug within 10 minutes and a total of 52% within the 5 day immersion period studied. PEO treated surfaces showed two-phase release kinetics where a short fast release phase was followed by a long-term slow release phase and was therefore modelled by means of a two-phase Fickian diffusion model ( $r = 0.99866$ ). The preliminary findings of this study indicate that PEO-treated NiTi surfaces have potential as PF drug carrier for DES.

---

Keywords: Drug Elution, Nitinol, Polymer-Free, 6-Mercaptopurine, Sustained Release

## 1 Introduction

Atherosclerosis is a disease characterised by the presence of an atheroma, which is a localised thickening of the arterial walls. The atheroma forms protrusions in the vessel lumen which disturb, and may also obstruct, proper blood flow if arterial spasms occur, or if a roaming blood clot tries to pass through (Khan *et al.* 2011, Marieb *et al.* 2010). DES are currently the treatment of choice for *de novo* lesions. The first generation of DES used permanent polymeric carriers for drug elution; however, these gave rise to high rates of late stent thrombosis and scar tissue formation. Alternative polymer-free approaches are now being investigated.

Nitinol has a number of advantages over conventional stent materials most of which derive from the material's superelasticity. Nitinol stents are self-expandable, and as such, do not require balloon deployment, resulting in less endothelial damage and lower crossing profile as well as more flexible stent delivery systems (Yoneyama *et al.* 2009). Although a number of polymer-free DESs are commercially available, none of the ones for coronary applications employ Nitinol stent backbones. Recent develop-

ments in this area of research have shown that Nitinol stents gave favourable results due to their low strut thickness, flexibility and chronic outward force. Nitinol has also shown good biocompatibility and corrosion resistance when in simulated body environments (Shabalovskaya *et al.* 2008, Thierry *et al.* 2002). Furthermore, its characteristic material properties have encouraged its use in complex lesions (such as bifurcations, vulnerable plaques, peripheral vessels, small vessels or superficial vessels) for which conventional materials did not perform well (Yoneyama *et al.* 2009). This trend has been seen in both BMSs and DESs, with an increasing interest in Nitinol over the years. However, no polymer free Nitinol DES are available for coronary applications.

In addition to the polymeric carriers, several researchers have suggested that the conventional antirestenotic drugs used in DES may also cause delayed re-endothelialisation (Puskas *et al.* 2009, Venkatraman *et al.* 2007). A quick evaluation of the main antirestenotic drugs currently being used reveals that the drugs are either cytotoxic or cytostatic. Due to the fact that the effects of these drugs are not cell type specific, achieving the necessary reduction in vascular smooth muscle cell

(VSMC) proliferation will also have deleterious effects on endothelial cell (EC) proliferation. This issue, although not free from controversies, has induced scientists to search for better drugs and bioactive agents which are able to promote endothelial healing while suppressing VSMC proliferation.

6-Mercaptopurine (6-MP) ( $C_5H_4N_4S$ ) is one such drug currently studied. Pires et al. (2007) and Pols et al. (2010), showed that local administration of 6-MP to hypercholesteremic transgenic mice results in increased protection against atherosclerosis development. Human VSMC proliferation was also inhibited during in vitro cell culture with 6-MP. Their findings revealed that 6-MP activates the nuclear receptor Nur77, both in vitro and in murine models, and inhibits neointima formation in the latter, without inducing vascular cell apoptosis. From their studies, the authors conclude that this drug is able to down-regulate VSMC and monocyte proliferation, while up-regulating EC proliferation – an ideal behaviour for an anti-restenotic drug. They therefore propose this drug as a novel drug to be used for the prevention of in-stent restenosis.

Most of the surface treatments applied to Nitinol to date have been focussed on improving the corrosion resistance, limiting nickel release and improving the biocompatibility. Nevertheless, recently micro-porous surfaces have been obtained by plasma electrolytic oxidation (PEO) by Huan *et al.* (2012). PEO is a surface modification technique, based on the anodic oxidation process, which operates at a voltage above the breakdown voltage of the oxide and therefore results in the occurrence of plasma micro-discharges along the surface immersed in the electrolyte. These micro-discharges lead to the formation of microporosity, spread over the oxide layer formed. The porous layer formed consists mainly of  $TiO_2$ , known for its biocompatibility. The porous topography of these surfaces makes them attractive for providing novel biofunctionality such as drug elution.

The aim of this study was to assess the potential of a microporous layer of  $TiO_2$  produced on Nitinol by means of EP+PEO treatment to act as a PF carrier for 6-MP, which is a novel anti-restenotic drug. Studies on the ability of Nitinol, with these surface modifications, to maintain a sustained release of drugs have not yet been published, making this area of study on the forefront of current research.

## 2 Materials and Methods

### 2.1 Material Used

The material used was a Ni-Ti alloy, with 50.7 atomic percent titanium and 49.3 atomic percent nickel. It was provided in the form of a sheet 85mm wide by 300mm long and 1mm thick. The material was cut into strips 1cm wide and 85mm long and a hole was drilled into one end of the strips to enable the attachment of electrical connectors during electrochemical processing. The strips were finally cleaned by ultrasonication for 10 minutes in isopropanol and deionised water, respectively, and stored in sterile sample bags.

### 2.2 Surface Treatment

#### 2.2.1 Electropolishing

Electropolishing (EP) was conducted in an electrolytic cell which consisted of a glass beaker with a volume of 120ml with a cylindrical stainless steel electrode. The cell was filled with 100ml of electrolyte which was a mixture of acetic acid ( $CH_3COOH$ ) and perchloric acid ( $HClO_4$ ) in the ratio 5:1 v/v, while stirring at 300rpm by means of a magnetic stirrer (Ika, Netherlands). The Ni-Ti strips were then screwed to an insulated metallic rod and suspended in the centre of the electrochemical cell, allowing only 1cm of the strip length to be in contact with the electrolyte. The metallic rod and the cylindrical steel electrode (which was surrounding the Ni-Ti strip in the cell), were then electrically connected to a potentiostat set to 10 V and left to run for 7 minutes for each sample. The Ni-Ti strip was removed and flushed with running water for 10 minutes. The Ni-Ti strips were then briefly rinsed in deionised water, dried with compressed air and stored in clean sample bags for further processing. Each batch of electrolyte was used to polish a maximum of 5 samples.

#### 2.2.2 Plasma Electrolytic Oxidation

Plasma electrolytic oxidation (PEO) was conducted in the same electrolytic cell used for electropolishing. The cell was filled with 100ml of frozen concentrated phosphoric acid ( $H_3PO_4$ ) as an electrolyte, while stirring at 300 rpm by means of a magnetic stirrer (Ika, Netherlands). The Ni-Ti strips were again screwed to an insulated metallic rod and suspended in the centre of the electrochemical cell, allowing only 1cm of the strip length to be in contact with the electrolyte. The metallic rod and the cylindrical steel counter electrode were then electrically connected to a galvanostat set to supply a current of 690mA (equivalent to

30A/dm<sup>2</sup> at the sample surface) and left to run until the voltage reached 55V. The Ni-Ti strip was removed and flushed with running water for 10 minutes. The treated Ni-Ti strips were then briefly rinsed in deionised water, dried with compressed air and stored in clean sample bags for further processing. Each batch of electrolyte was used to treat a maximum of 4 samples, in order for it not to overheat. The electrolyte was therefore refreshed and the used electrolyte was returned to the freezer, to be reused after a few hours of cooling.

## 2.3 Surface Characterization

### 2.3.1 Scanning Electron Microscopy and Energy Dispersive Spectroscopy

The surfaces of the EP and EP+PEO samples were examined by scanning electron microscopy (SEM, JSM-6500F, JEOL) using an accelerating voltage of 5 kV. Before imaging, the EP+PEO samples were sputter coated with carbon to enhance their conductivity. The elemental composition was estimated on the surface by means of an energy dispersive X-ray spectrometer (EDS, INCA Energy, Oxford Instruments) coupled with the SEM equipment.

The samples were first observed and photographed at various magnifications in the range of 50 to 10,000 times and elemental analysis was carried out at the latter magnification. Imaging and EDS analysis were performed at three different locations on the supplied samples in order to have a good overview of how the surface morphology of the samples varies and to be able to calculate the average composition of the alloy.

### 2.3.2 Roughness Measurement

Three samples were used for each type of surface finish and five repetitions of the measurements were conducted on each sample. The samples were placed on a flat surface and their roughness was measured by means of a Surtronic 3+ surface roughness tester. Due to the small size of the samples (only 1cm square) it was impossible to hold them in position manually during testing. It was therefore necessary to stick them to the testing table by means of double sided adhesive tape, ensuring that they were well attached to the tape in order to avoid any motion of the samples during testing. All the parameters measured by the device were recorded and their average values and standard deviations were calculated for each sample subset.

### 2.3.3 Hydrophilicity

The samples were cleaned by ultrasonication for 5 minutes in 70% ethanol and deionised water, respectively and dried in compressed air. The instrument which was used to measure the contact angle was a Kruss Drop Analyser 100. The software of the machine was set to perform dynamic measurement thus taking 48 measurements of the contact angle in 48 seconds while the machine ejected 10µl of HPLC grade water onto the surface of the material and performed in triplicate. This process was repeated with diiodomethane for all samples in order to enable the calculation of the surface free energy according to Fowke's theory.

## 2.4 Drug Loading

### 2.4.1 6-MP Solution Preparation

250ml of 1.1mg/ml 6-MP stock solution were produced by following the ensuing procedure: 313.7 mg of 98% 6-mercaptopurine monohydrate were weighed and dissolved in 25ml of 0.1M NaOH solution. The solution was stirred by means of a magnetic stirrer until all the drug had dissolved. The remaining 225ml of deionised water were then added to the solution and stirring was continued for a further 10 minutes in order to ensure the solution was homogeneous.

### 2.4.2 Drug Spraying

The configuration of a BUCHI B-290 Spray dryer was modified in order to enable drug spraying. The device was connected to an external spray nozzle and a drip catch, with a perforated glass plate, was clamped under the nozzle in order to act as a sample holder while allowing excess drug solution to drain and be collected in a flat bottomed flask.

The drip catch was fixed at a distance from the nozzle which minimised the interaction of the drip catch walls with the spray cone, while maximizing the area on the glass plate which was being wet homogeneously by the spray cone at the chosen gas flow rates. During drug spraying, the samples were placed within the latter mentioned area, keeping the same position for each spray cycle, in order to limit inter-sample variability.

The 6-MP stock solution was placed in a beaker, stirred at 200rpm by means of a magnetic stirrer and fed to the peristaltic pump. The nitrogen flow rate was set to 192L/hr and the peristaltic pump was switched on at 29ml/hr and left to run for 10 seconds per spray cycle. The drug coated sample was then removed from within the drip catch by means of long twee-



zers, placed on absorbent paper and left to dry under a warm blower in a fume cabinet for a couple of minutes. The process was repeated 20 times and after the final drying step the samples were briefly rinsed in 30% ethanol and dried again

### 2.4.3 Drug Load Determination

In order to determine the amount of drug loaded onto the surfaces of the samples, the loaded samples were immersed in amber bottles containing 8ml of deionised water and 2ml of 0.1M HCl to limit drug degradation. These bottles were then ultrasonicated for three hours, shaken vigorously, left to shake in an immersion bath at 37°C for 21 hours, and again shaken vigorously. Samples of 1ml were extracted from the bottles after three hours and 24 hours, placed in capped 1.5ml eppendorf tubes and stored at -18°C to avoid drug degradation before drug content evaluation by HPLC analysis. Three samples were used for each sample set in order to enable the calculation of the average drug load and standard deviation. Drug loading efficiency was calculated as the percentage of 6-MP still present on the surface after rinsing of drug coated samples.

### 2.5 *In vitro* 6-MP Release

The drug coated samples were immersed in amber glass bottles holding 10 ml of Phosphate Buffered Saline (PBS) containing 25mM hydrochloric acid (HCl) (to halt drug degradation) in an incubator at 37°C, under shaking conditions. At each sampling time point, the bottles were shaken gently and the NiTi samples were removed by means of tweezers and placed in the caps of the bottles. The bottles were shaken once again, a 0.5ml sample of the release medium was extracted and the NiTi samples were placed back into the bottle. The samples extracted were placed in capped 1.5 ml eppendorf tubes together with 0.5ml of deionised water and stored at -18°C to avoid the occurrence of drug degradation before drug content evaluation by HPLC analysis.

## 2.6 High Performance Liquid Chromatography (HPLC)

### 2.6.1 Preparation of Standard Mixtures

A stock solution of 6-MP at a concentration of 200µg/ml was prepared by dissolving the appropriate amount of 6-mercaptopurine monohydrate (98%) in 1ml of 0.1M NaOH, diluting with 22ml of deionised water and acidifying with 2ml of 0.1M HCl. The stock solution was then used to produce five standard mixtures containing 0.1 µg/ml, 0.5 µg/ml, 1 µg/ml, 5

µg/ml and 10 µg/ml of 6-MP, by diluting with deionised water as appropriate. Aliquots of 1ml of these standard mixtures were placed in capped 1.5ml eppendorf tubes and stored at -18°C to avoid the occurrence of drug degradation before HPLC analysis.

### 2.6.2 HPLC Analysis

The 6-MP content of standard mixtures and experimental samples was determined by means of a Varian Prostar HPLC equipped with a mobile phase delivery system and a Chromospheres C18 reversed-phase column (250 x 4.6mm, 5µm particle size). The concentration of 6-MP present in each sample was determined using a Varian Prostar spectrometer reading at 322 nm, with a retention time of 3.6 minutes. The eluent used was a mixture of 7.5: 92.5 (v/v) methanol – water containing 100mM triethylamine and adjusted to pH 3.2 by means of concentrated phosphoric acid. The eluent was filtered and pumped through the machine at a flow rate of 1ml/min, activating the pump at least 30 minutes before the start of the analysis to ensure the system had been adequately purged from any contaminants. The machine was calibrated every day of use by analysing vials containing the five standard mixtures described earlier and a vial containing deionised water. All the results presented are the average values obtained from at least 3 replicates.

## 2.7 Mathematical Modelling of Drug Release

In order to better characterise the release kinetics observed for EP+PEO samples, the data obtained was fitted by means of two models: Korsmeyer-Peppas model and a two-phase elution model based on Ficks' first law of diffusion. The fit of these models to the experimental data was evaluated by calculating the Pearson product moment correlation coefficient ( $r$ ) which tends to 1 with increasing correlation.

The Korsmeyer-Peppas model is a power law which takes the form of:

$$\frac{M(t)}{M_{\infty}} = kt^n \dots (1)$$

where  $M(t)$  is the accumulated released mass at time  $t$ ,  $M_{\infty}$  is the total amount of drug loaded on the surface which would be released at  $t \rightarrow \infty$ ,  $k$  is the kinetic constant and  $n$  is the release exponent (Moseke 2012). In thin films, when  $n \leq 0.5$ , the release of the drug is diffusion based, and when  $0.5 < n \leq 1$ , it is degradation based.

In this model  $M_{\infty}$  can be measured experimentally and  $k$  and  $n$  can be extrapolated from the experimental data. If logs to base  $e$  are taken on both sides of equation 4 we get:

$$\ln \frac{M(t)}{M_{\infty}} = \ln k + n \ln t \quad \dots (2)$$

Therefore, by applying the natural logarithm to the experimental data and fitting a straight line to this data it is possible to obtain  $n$  and  $k$ .

Due to the fact that the data obtained experimentally exhibited a two-phase release behaviour, a two-phase release model was also used to approximate the release kinetics observed. In this model the release is assumed to be based on a fast release phase and a slow release phase, both of which are based on first-order release kinetics. Assuming that the two release phases are independent from each other, the two-phase model therefore has the form:

$$M(t) = M_{\infty} - M_f \cdot e^{-C_f t} - M_s \cdot e^{-C_s t} \quad \dots (3)$$

where  $M(t)$  is the accumulated released mass at time  $t$ ,  $M_{\infty}$  is the total amount of drug loaded on the surface which would be released at  $t \rightarrow \infty$ ,  $M_s$  is the mass available for slow release,  $M_f$  is the mass available for slow release, and  $C_s$  and  $C_f$  are the first-order kinetic constants for slow and fast release respectively (Peng 2009).

Furthermore, it is known that  $M_{\infty} = M_f + M_s$ , therefore by identifying the transition between fast and slow release it is possible to determine  $M_f$  and  $M_s$ . Moreover,  $C_s$  and  $C_f$  can be calculated from the experimental data by considering the first and the last few data points obtained in the experimental data.

### 3 Results and Discussion

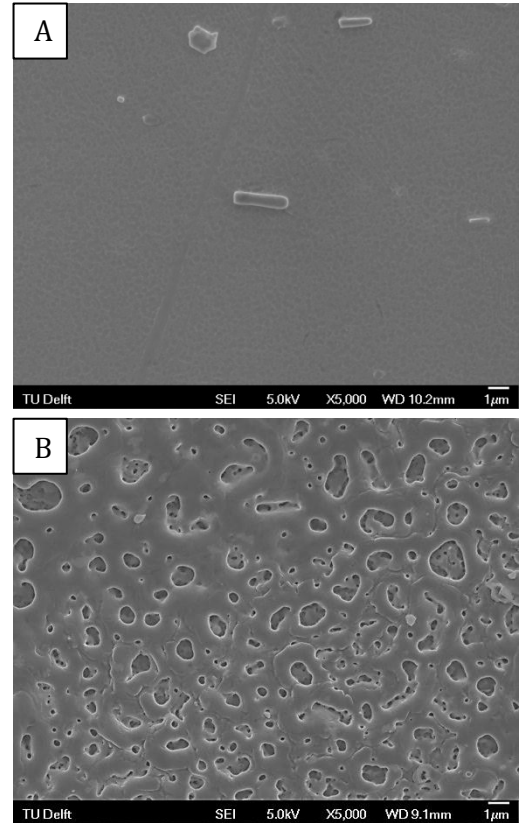
#### 3.1 Surface Characterization

##### 3.1.1 Surface Morphology

The surface morphologies of EP and EP+PEO treated samples, as evidenced by SEM can be seen in Figure 1.

In Figure 1A it can be observed that the surface of the electropolished samples is rather smooth with some inclusions visible at the surface. These inclusions, however, do not remain visible when such samples undergo PEO treatment, as seen in Figure 1B. The latter image evidences that the PEO treatment gave rise to the formation of surface porosity with pore size varying between a couple of microns

to a couple of tenths of a micron in diameter. Further, the larger pores are connected to the finer porosity within them, that extends deeper into the titania layer.



**FIGURE 1 – SEM IMAGES (5000x) OF SURFACE MORPHOLOGIES OF NiTi: (A) EP SAMPLES AND (B) EP+PEO SAMPLES.**

The elemental composition of the surfaces of EP and EP+PEO treated samples was analysed by means of EDS. The results obtained were tabulated and presented in Table 1.

**TABLE 1 – MEAN ELEMENTAL COMPOSITIONS OBTAINED BY EDS ANALYSIS**

Sample	Atom (% ±SD)				Ni/Ti (±SD)
	Ni	Ti	O	P	
EP	49.65 ± 0.27	50.35 ± 0.27	—	—	0.99 ± 0.01
EP+PEO	9.03 ± 0.13	18.55 ± 1.40	52.58 ± 0.97	19.84 ± 0.54	0.49 ± 0.03

Once the material undergoes PEO treatment, the surface composition changes significantly. This is due to the formation of a layer of oxide on the surface and the uptake of phosphorus from the electrolyte. Moreover, since the oxidation of titanium is more thermodynamically favorable than that of nickel (Shabalovskaya *et al.* 2008), it oxidises in preference to it, thus causing a decrease in the ratio of nickel to titanium. Furthermore, it is observed that EP results in a more homogenous surface, bringing

about a lower standard deviation in the composition when PEO is preceded by EP (please refer to data presented in Table 3 of the report).

### 3.1.2 Surface Porosity

As described previously, SEM images of the EP+PEO samples were used in order to characterise surface porosity. From the analysis conducted it was calculated that the average porosity was 9.9%, the average pore density was  $1.04 \text{ pores}/\mu\text{m}^2$ , the average pore diameter was  $0.36 \mu\text{m}$  and the average pore area was  $0.11 \mu\text{m}^2$ . The results obtained are illustrated in Figure 2, where the bar shows the average value calculated and the error bars represent the standard deviation of each value. These results are important to identify which factors will be playing a role during drug elution. When comparing the pore diameter to the molecular diameter of 6-MP (which is about 1.6 nm, assuming the molecule is spherical) we conclude that the interaction of the molecule with the pore walls will not have a significant effect on the rate of diffusion.

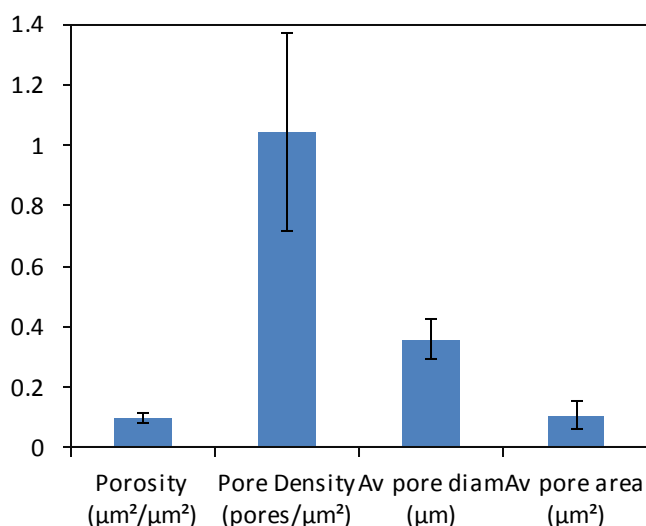


FIGURE 2— POROSITY CHARACTERISTICS FOR EP+PEO SAMPLES. ERROR BARS REPRESENT THE STANDARD DEVIATION FROM THE MEAN VALUE.

### 3.1.3 Surface Roughness and Hydrophilicity

The Ra values obtained for EP and EP+PEO samples were found to be  $0.135 \pm 0.04 \mu\text{m}$  and  $0.191 \pm 0.05 \mu\text{m}$ , respectively. The roughness therefore does not change significantly upon PEO treatment due to the large standard deviation for both surfaces.

The average water contact angles for EP and EP+PEO surfaces were found to be  $28.71 \pm 0.59^\circ$  and  $11.21 \pm 0.91^\circ$  respectively and the

surface energies for these surfaces were calculated to be  $67.29 \pm 1.12 \text{ mJ/m}^2$  and  $74.41 \pm 0.39 \text{ mJ/m}^2$  respectively. The findings clearly show that the surface treatment of the samples caused a change in the surface chemistry and an increase in specific surface area, resulting in significant changes in the hydrophilicity of the surface. In our case, a decrease in water contact angle is beneficial since it points towards better cell compatibility and spreading once the stents are implanted. Furthermore, since the drug spraying solution is water based, a lower water contact angle results in better spreading of the drug on the surface and possibly also better infiltration of the drug within the surface porosity present on EP+PEO surfaces.

## 3.2 Drug Loading and Release

### 3.2.1 Effect of PEO Treatment on Drug Loading

The only Nitinol, polymer-free drug eluting stent currently available on the market is the Zilver PTX. The final surface of this stent is electropolished and is loaded with Paclitaxel without the use of any binders or polymers. The differences in drug loading potential of EP and EP+PEO treated samples were therefore studied and the results obtained are presented in Figure 3.

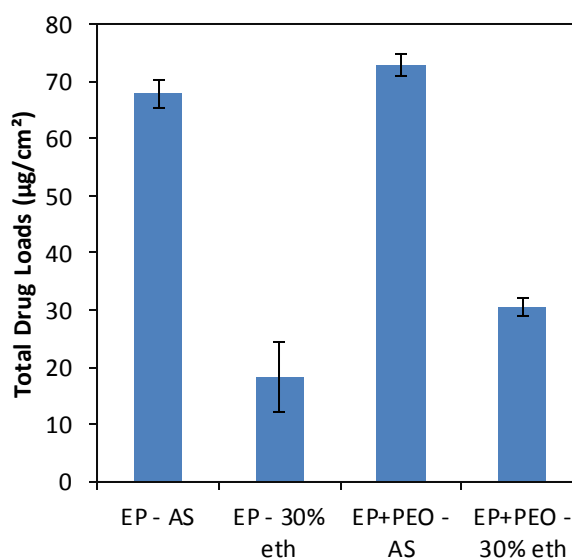


FIGURE 3 – MEAN DRUG LOADS OF SPRAY 20 EP AND EP+PEO SAMPLES, WITH OR WITHOUT RINSING IN 30% ETHANOL ( $N \geq 4$ ). ERROR BARS REPRESENT THE STANDARD DEVIATION FROM THE MEAN.

The surfaces considered here have been coated by 20 layers (Spray 20) of sprayed drug solution at a gas flow rate of 192 L/hr, with and without final rinsing. This data shows that EP+PEO surfaces were able to retain a significantly higher amount of drug during spraying.



During drying the drug had a tendency to slide off the smooth electropolished surfaces. On the other hand, the porosity present on EP+PEO surfaces seems to act as a drug reservoir, resulting in higher final drug loads. Further, the drug load remained higher for EP+PEO samples after rinsing. This is confirmed by calculating the drug loading efficiency of the two surfaces. While EP surfaces have a drug loading efficiency of 26.8%, EP+ PEO surfaces exhibit an efficiency of 41.9%. A typical SEM image of the drug distribution within the surface porosity and the EDS spectrum from the crystals within the pores is shown in Figure 4. The presence of sulphur indicates that the crystals seen are 6-MP.

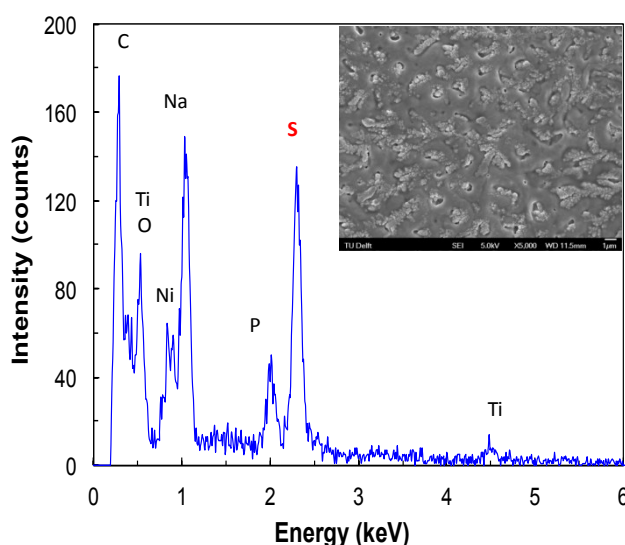


FIGURE 4 – EDS ANALYSIS OF THE LOADED EP+PEO SURFACES. THE INSET REPRESENTS THE SEM IMAGE OF A TYPICAL PEO TREATED SURFACE LOADED WITH 6-MP.

Literature data suggests that in most cases the drug loads are in the range of 100-200 $\mu\text{g}/\text{cm}^2$  (Garg *et al.* 2010). Although the optimal dose of 6-MP is yet to be established, ways to increase the amount of 6-MP need to be further explored. These include the surface characteristics, the drug loading method, the loading conditions chosen and the solvent type. Use of organic solvents with lower surface contact angles on EP+PEO samples might give the desired results when coupled with optimised drug loading and drying conditions.

### 3.2.2 Effect of PEO Treatment on the *In Vitro* 6-MP Release

The release profiles obtained from EP and EP+PEO surfaces in acidified PBS at 37°C, under shaking conditions are shown in Figure 5. The PBS has been acidified in order to sup-

press 6-MP degradation (please see the results on drug stability in the report, p. 36).

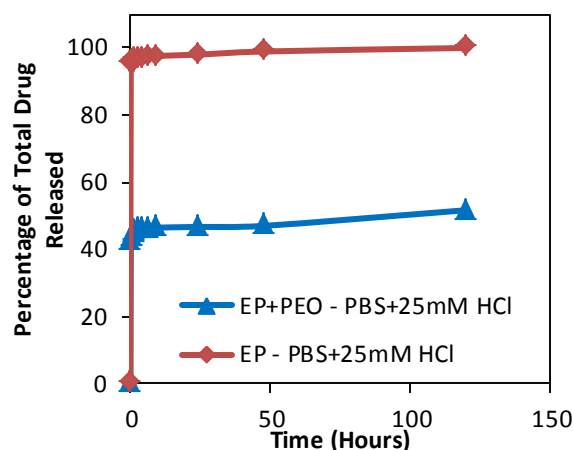


FIGURE 5 – 6-MP RELEASE IN PBS + 25mM HCl AT 37°C DURING THE FIRST 120 HOURS OF IMMERSION FROM EP AND EP+PEO SAMPLES LOADED BY DRUG SPRAYING 20 LAYERS AT A GAS FLOW RATE OF 192L/HR WITH 30% ETHANOL FINAL RINSING.

The release profile of EP+PEO shows two distinct phases: a burst phase in the first 10 minutes when about 42% of the drug is released at an average rate of 1.3 $\mu\text{g}/\text{min}$ , followed by a slow release thereafter at an average rate of 0.0153 $\mu\text{g}/\text{min}$ . At the end of the 5 day period the total percentage of drug released was 52%. In contrast, EP samples released most ( $\approx 95\%$ ) of the loaded drug within the first 10 minutes of immersion. This highlights the superiority of PEO treated surfaces over EP treated surfaces in sustaining the release of 6-MP. This superiority is derived from the micropores produced during PEO treatment which act as drug reservoirs, away from the immediate surface of the material. The drug must therefore first dissolve and then diffuse through the porosity in order to be released to the surrounding medium, making the solubility of the drug a determining parameter for the rate of release.

The advantages of the EP+PEO surfaces studied are highlighted further when we compare the release kinetics obtained with those for the Zilver PTX and the Yukon found in literature. The Zilver PTX releases 98% of the Paclitaxel drug within 24 hours (*in vivo*) (FDA executive report) while the Yukon stent releases 70-80% of Sirolimus (*in vitro*) in 5 days (www.translumina.de). The EP+PEO surfaces therefore release a lower percentage of the loaded drug than the latter in the same period of time, notwithstanding the fact that the solu-

bility of Sirolimus is two orders of magnitude lower than that of 6-MP (Beuch *et al.* 2007).

### 3.3 Mathematical Modelling of Drug Elution

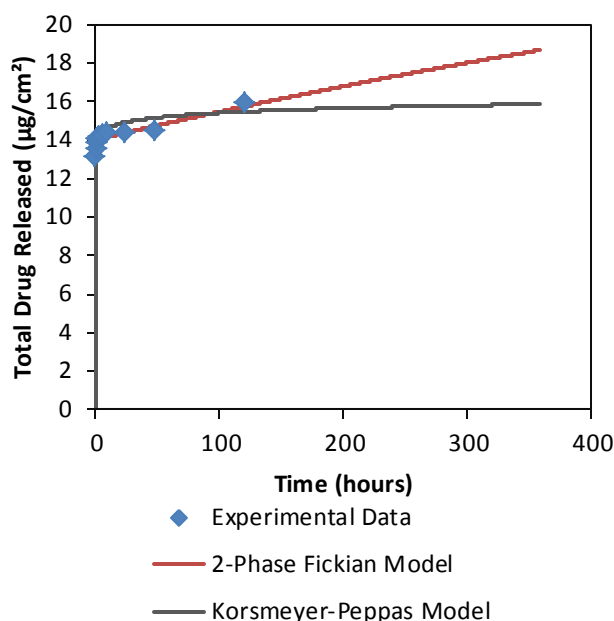
In order to better characterise the release kinetics observed for EP+PEO samples, the data obtained was fitted by means of two models used in literature for the simulation of drug release from polymer-free surfaces: the Korsmeyer-Peppas model (Moseke 2012) and a two-phase elution model based on Ficks' first law of diffusion (Peng 2009). The constants required for the two models described previously were calculated and tabulated in Table 2.

**TABLE 2 – CONSTANTS USED FOR DRUG RELEASE MODEL DEVELOPMENT**

Common	Korsmeyer-Peppas		2-Phase Fickian			
$M_{\infty}$	$k$	$n$	$M_f$	$M_s$	$C_f$	$C_s$
30.6000	0.4542	0.0227	13.4300	16.5700	3.3214	0.0009

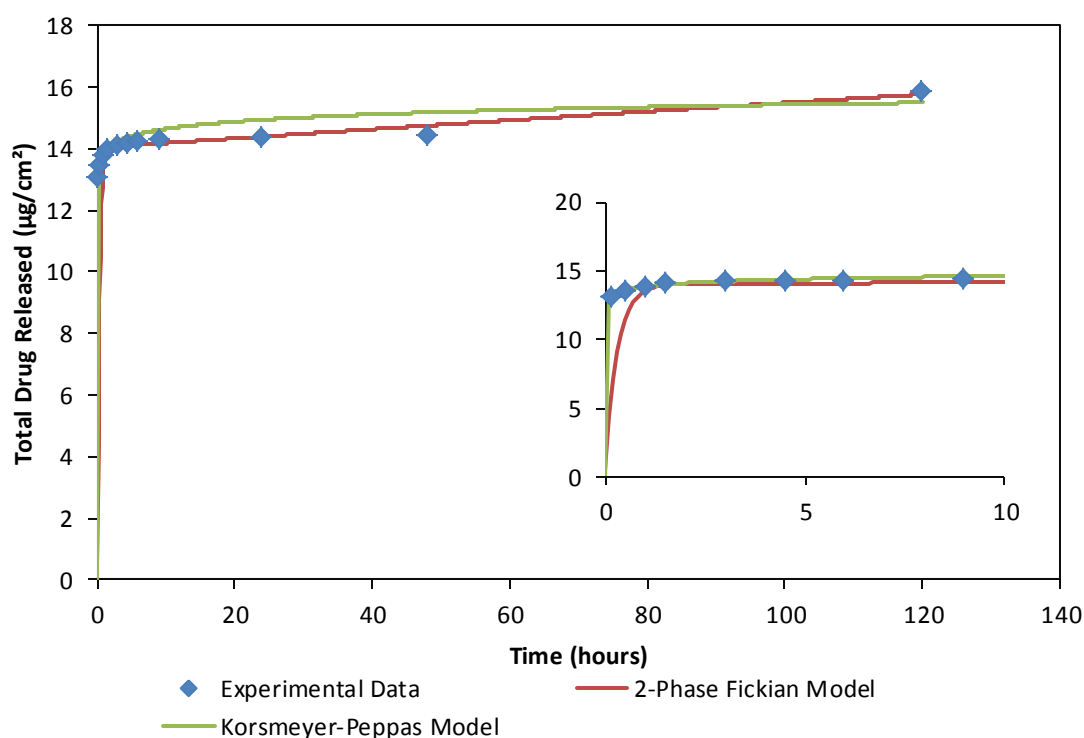
The data for the models of drug release kinetics chosen was therefore generated and plotted with the experimental data in Figure 7. The  $r$  values for the two-phase Fickian and the Korsmeyer-Peppas model data sets compared to the experimental data were 0.99866 and

0.999953 respectively. This shows that both models gave a good fit to the data.



**FIGURE 6 – MODEL EXTRAPOLATION TO 360 HOURS OF RELEASE IN COMPARISON TO EXPERIMENTAL DATA FOR FIRST 120 HOURS OF RELEASE.**

Although both models gave a good fit, the data plotted in Figure 7 seems to suggest that the 2-Phase Fickian model gives a better fit to the two-phase release measured experimentally. A



**FIGURE 7 – COMPARISON OF RELEASE KINETICS MODELS TO AVERAGE EXPERIMENTAL (N=3) 6-MP RELEASE DATA IN PBS + 25mM HCl AT 37°C DURING THE FIRST 120 HOURS OF IMMERSION FROM EP+PEO SAMPLES LOADED BY DRUG SPRAYING 20 LAYERS AT A GAS FLOW RATE OF 192L/HR WITH 30% ETHANOL FINAL RINSING. INSERT SHOWING ENLARGED INITIAL 10 HOUR PORTION.**

closer look at the fitting curves (insert Figure 6) indicates that during the initial phases of release (burst) the Korsmeyer-Peppas model gives a very good fit. However, since the main aim of the PEO treated Nitinol is to provide a sustained release of the drug over longer periods of time, the model was extrapolated to 360 hours (Figure 6). Here it becomes evident that the Korsmeyer-Peppas model does not describe the release kinetics adequately since it is known that the average total load of 6-MP is  $30.6\mu\text{g}/\text{cm}^2$  and the release predicted by this model seems to flatten out. Future work should therefore extend the experimental release period further in order to be able to assess whether the two-phase Fickian model gives an adequate approximation of the release kinetics involved.

## 4 Conclusions

This study dealt with the assessment of the potential of PEO treated NiTi surfaces to sustain the release of the novel anti-restenotic drug 6-MP. A microporous titania layer was created on the surface of Nitinol samples by means of EP followed by PEO. SEM analysis showed a wide range of pore diameters varying from a couple of microns to a couple of tenths of a micron, with an average pore diameter of  $0.36\mu\text{m}$ . Furthermore, it was seen that this treatment gave rise to a decrease in the water contact angle from  $28.71 \pm 0.59^\circ$  in the EP material to  $11.21 \pm 0.91^\circ$  but caused no significant differences in the surface roughness.

EP and EP+PEO treated surfaces were loaded with 6-MP by spraying 20 layers of an aqueous solution of the drug with intermediate drying and a final rinsing step in 30% ethanol. An average of  $18.2\mu\text{g}/\text{cm}^2$  and  $30.6\mu\text{g}/\text{cm}^2$  of 6-MP was loaded on the EP and EP+PEO samples respectively. Further, the drug loading efficiency for EP+PEO surfaces was 41.9% while that for EP surfaces was just 26.8%. The release of 6-MP from EP+PEO surfaces in acidified PBS at  $37^\circ\text{C}$  showed a burst release (42%) followed by a slow sustained release of the drug over the following 5 days of immersion, at the end of which 52% of the loaded drug had been released. In comparison, EP surfaces showed a release of 95% of the loaded drug within the first 10 minutes of immersion.

The experimental data collected for EP+PEO samples was compared to two models of drug release kinetics based on diffusion; namely, a two-phase Fickian diffusion model and the Korsmeyer-Peppas model. Although both mod-

els showed a good fit, the extrapolation of the data to extended times suggested that the two-phase Fickian diffusion model gave results which were closer to the ones expected. Further validation of this model must however be conducted by extending the experimental release period.

The results suggest the potential of PEO-treated surfaces as drug reservoirs and for the sustained release of 6-MP.

## 5 References

- Buech, G., Bertelmann, E., Pleyer, U., Siebenbrodt, I., Borchert, H.H., 2007. Formulation of sirolimus eye drops and corneal permeation studies. *Journal of Ocular Pharmacology and Therapeutics*, 23(3), pp.292-303
- Curran, J.A. and Clyne, T.W., 2006. Porosity in plasma electrolytic oxide coatings. *Acta Materialia*, 54, pp. 1985-1996.
- Dong, H., 2010. *Surface Engineering of Light Alloys – Aluminium, magnesium and titanium alloys*, Woodhead Publishing Limited, CRC Press.
- Garg, S. and Serruys, P.W., 2010. Coronary stents – Looking forward. *Journal of the American College of Cardiology*, 56(10), pp. S43-S78.
- Huan, Z., Fratila-Apachitei, L.E., Apachitei, I., Duszczek, J., 2012. Porous NiTi surfaces for biomedical applications. *Applied Surface Science*, 258, pp. 5244-5249.
- Khan, M.G., 2011. *Encyclopedia of Heart Disease*. 2<sup>nd</sup> Ed. Humana Press, Springer Reference.
- Marieb E.N., Hoehn, K., 2010. *Human anatomy and Physiology*, 8<sup>th</sup> edition, Pearson international edition, pp. 694-751.
- Moseke, C., Hage, F., Vorndran, E., Gbureck, U., 2012. TiO<sub>2</sub> nanotube arrays deposited on Ti substrate by anodic oxidation and their potential as a long-term drug delivery system for antimicrobial agents. *Applied Surface Science*, 258, pp. 5399-5404.
- Peng, L., Mendelsohn, A.D., LaTempa, T.J., Yoriya, S., Grimes, C.A., Desai, T.A., 2009. Long term small molecule and protein elution from TiO<sub>2</sub> nanotubes. *Nano Letters*, 9(5), pp.1932-1936.
- Pires, N.M.M., Pols, T.W.H., de Vries, M.R., van Tiel, C.M., Bonta, P.I., Vos, M., Arken-

bout, E.K., Pannekoek, H., Jukema, J.W., Quax, P.H.A., de Vries, C.J.M., 2007. Activation of Nuclear Receptor Nur77 by 6-Mercaptopurine Protects Against Neointima Formation. *Circulation*, 115, pp. 493-500.

Pols, T.W.H., Bonta, P.I., Pires, N.M., Otermin, I., Vos, M., de Vries, M.R., van Eijk, M., Roelofsen, J., Havekes, L.M., Quax, P.H., van Kuilenburg, A.B.P., de Waard, V., Pannekoek, H., de Vries, C.J.M., 2010. 6-Mercaptopurine Inhibits Atherosclerosis in Apolipoprotein E\*3-Leiden Transgenic Mice Through Atheroprotective Actions on Monocytes and Macrophages. *Arteriosclerosis, Thrombosis and Vascular Biology*, 30, pp.1591-1597.

Puskas, J.E., Muñoz-Robledo, L.G., Hoerr, R.A., Foley, J., Schmidt, S.P., Evancho-Chapman, M., Dong, J., Frethem, C. Haugstad, G., 2009. Drug-eluting stent coatings. *WIREs Nanomedicine and Nanobiotechnology*, 1, pp. 452-462.

Shabalovskaya, S., Anderegg, J., van Humbeeck, J., 2008. Critical overview of Nitinol surfaces and their modifications for medical applications. *Acta Biomaterialia*, 4, pp.446-467.

Thierry, B., Merhi, Y., Bilodeau, L., Trépanier, C., Tabrizian, M., 2002. Nitinol versus stainless steel stents: acute thrombogenicity study in an ex vivo porcine model. *Biomaterials*, 23, pp. 2997-3005.

Venkatraman, S., Boey, F., 2007. Release profiles in drug eluting stents: Issues and uncertainties. *Journal of Controlled Release*, 120, pp.149-160.

Yoneyama T., Miyazaki, S., 2009. *Shape memory alloys for biomedical applications*, Woodhead Publishing Limited, CRC Press.



# **NITINOL DRUG ELUTING SURFACES FOR CORONARY STENTS**

---

## **PART II: THESIS REPORT**



## LIST OF FIGURES

Figure 1 – SEM images of the surface characteristics of the Yukon stent before and after drug loading. ....	2
Figure 2 – Molecular structure of 6-MP. ....	4
Figure 3 – Set-up used for drug spraying. (a) full view, (b) close-up of spraying nozzle. ....	12
Figure 4 – Typical HPLC chromatogram for 6-MP.....	16
Figure 5 – SEM images (5000x) of surface morphologies of NiTi samples (A) as-received, (B) electropolished, (C) PEO treated, (D) electropolished and PEO treated	19
Figure 6 – Porosity characteristics for PEO and EP+PEO samples, error bars representing the standard deviation of each value. ....	21
Figure 7 – Mean Ra measurements for as-received (AR), electropolished (EP), plasma electrolytic oxidation treated (PEO), and electropolished and PEO treated (EP+PEO) samples. Error bars represent the standard deviation from the mean value in the sample set tested.....	21
Figure 8 – Water contact angle average values for AR, EP, PEO and EP+PEO samples. Error bars represent the standard deviation of the average values measured. ....	23
Figure 9 – Total 6-MP release in PBS at 37°C after 6 hours from EP+PEO samples loaded by immersion and drug spraying at 138L/hr and 192L/hr gas flow. ....	24
Figure 10 – SEM images of the surface of EP+PEO samples after spraying 6 layers of 6-MP solution at 192 L/hr and rinsing in 50% ethanol. (A) 100X mag, (B) 10,000X mag at the centre of the sample, and (C) 10,000X mag at the edge of the sample. ....	25
Figure 11 – SEM images of the surface of EP+PEO samples after spraying 10 layers of 6-MP solution at 192 L/hr and rinsing in 50% ethanol. (A) 100X mag, (B) 10,000X mag at the centre of the sample, and (C) 10,000X mag at the edge of the sample. ....	26
Figure 12 – SEM images of the surface of EP+PEO samples after spraying 20 layers of 6-MP solution at 192 L/hr and rinsing in 50% ethanol. (A) 100X mag, (B) 5,000X mag at the centre of the sample, and (C) 5,000X mag at the edge of the sample. ....	27
Figure 13 – EDS spectrum obtained from crystals formed on the surface of EP+PEO samples after spraying 20 layers of 6-MP at 192 L/hr and rinsing in 50% ethanol. ....	28

Figure 14 – SEM images of the surface of EP+PEO samples after spraying 20 layers of 6-MP solution at 192 L/hr and rinsing in water: (A) 100x mag, (B) 10,000x mag.....	28
Figure 15 – SEM images of the surface of EP+PEO samples after spraying 20 layers of 6-MP solution at 192 L/hr and rinsing in 30% ethanol: (A) 100x mag, (B) 10,000x mag. ....	29
Figure 16 – SEM images of the surface of EP+PEO samples after spraying 20 layers of 6-MP solution at 192 L/hr. (A) 100X mag, (B) 10,000X mag at the centre of the sample, and (C) 5,000X mag at the edge of the sample. ....	30
Figure 17 – Total drug released after 6 hours of immersion in PBS at 37°C for rinsed(R) Spray 6 (50% ethanol) and Spray 20 (30% ethanol) samples compared to as-sprayed (AS) spray 20 samples. ....	30
Figure 18 – Mean drug loads present on Spray 20 EP and EP+PEO samples, with or without rinsing in 30% ethanol (n≥4). Error bars represent the standard deviation from the mean. ....	32
Figure 19 – 6-MP release in PBS at 37°C during the first 120 hours from EP+PEO samples loaded by drug spraying 20 layers at 192L/hr, with 30% ethanol rinsing. ....	33
Figure 20 – 6-MP release in PBS at 37°C during the first 6 hours from EP+PEO samples loaded by drug spraying 20 layers at 192L/hr, with 30% ethanol rinsing. ....	34
Figure 21 – Degradation of 6-MP at 37°C in various release media, over a 30 day period.....	35
Figure 22 – 6-MP release in PBS and PBS + 25mM HCl at 37°C during the first 120 hours of immersion from EP and EP+PEO samples loaded by drug spraying 20 layers at a gas flow rate of 192L/hr with 30% ethanol final rinsing. Insert showing enlarged initial 10 hour portion. ....	36
Figure 23 – SEM images of the surface of EP+PEO samples after release in (A) highly acidified PBS and (B) Acidified PBS .....	37
Figure 24 – Comparison of release kintetics models to experimental 6-MP release data in PBS + 25mM HCl at 37°C during the first 120 hours of immersion from EP+PEO samples loaded by drug spraying 20 layers at a gas flow rate of 192L/hr with 30% ethanol final rinsing. Insert showing enlarged initial 10 hour portion. ....	40
Figure 25 – Model extrapolation to 360 hours of release in comparison to experimental data for first 120 hours of release. ....	41



## LIST OF TABLES

Table 1 – Overview of currently available Nitinol DESs grouped according to application. ....	3
Table 2 – Standard values for polar and dispersive components of liquids used. ....	10
Table 3 – Mean elemental compositions obtained by EDS analysis.....	20
Table 4 – Measured water and diiodomethane contact angles and calculated surface free energy for the four surfaces tested. ....	22
Table 5 – Solubility of 6-MP in various solvents .....	23
Table 6 – Solutions Employed for the Study of 6-MP Stability .....	35
Table 7 – Constants used for drug release model development.....	39

## LIST OF ABBREVIATIONS

6-MP – 6-Mercaptopurine

AR – As-received

AS – As-sprayed

CVD – Cardiovascular diseases

DES – Drug eluting stents

EC – Endothelial cells

EDS – Energy dispersive spectroscopy

EP – Electropolishing

EP+PEO – Electropolishing followed by plasma electrolytic oxidation

HPLC – High performance liquid chromatography

ISR – In-stent restenosis

NiTi – Nitinol

PEO – Plasma electrolytic oxidation

SEM – Scanning electron microscope

TNT – Titania nanotubes

VSMC – Vascular smooth muscle cells

# 1. INTRODUCTION

---



# 1 INTRODUCTION

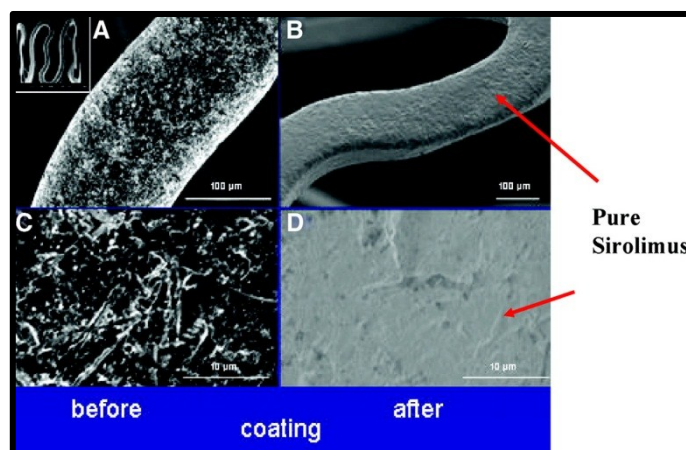
## 1.1 BACKGROUND

Cardiovascular diseases (CVD) are the cause of about 40% of the deaths occurring in westernised societies, making them the leading cause of death in today's societies (Khan *et al.* 2011). CVD however are also the cause of disabilities, making the costs and loss in quality of life associated with this set of diseases some of the highest of our days. Atherosclerosis forms the basis for CVD, resulting in formation of localised thickenings of the arterial walls, also known as atheroma or plaques, which disturb blood flow and thus may also easily result in myocardial infarction or stroke (Khan *et al.* 2011, Marieb *et al.* 2010). The development of this disease is caused by a large number of environmental and genetic factors which are difficult to control and therefore treatment has mostly been focussed on dealing with the final effects of the disease rather than the prevention of its occurrence altogether. Current treatment options for atherosclerosis include vascular grafting, balloon angioplasty and vascular stenting (Kutz *et al.* 2009). Nowadays however, vascular grafting is only used as a last option since balloon angioplasty and vascular stenting have brought about great improvements in success rates and the possibility for "revision" if restenosis of the vessels occurs. Relatively high rates of restenosis are however still encountered with balloon angioplasty and bare metal stents, leading the way to the use of drug eluting stents, which have become the treatment of choice for *de novo* lesions.

Conventional drug eluting stents (DES) were made up of a metallic backbone (stainless steel, cobalt chromium alloy or nickel titanium alloy) which was coated with a non-degradable polymeric film (one layer or a combination of layers to modulate the drug release) that released anti-proliferative drugs (Sirolimus and Tacrolimus) in order to prevent restenosis. The main problem with this approach was that the long term presence of polymeric films gave rise to late stent thrombosis and caused inflammation and incomplete healing in the surrounding tissue (Kukreja *et al.* 2008). This led to the development of DES with biodegradable polymeric films to avoid late stent thrombosis; however, the problems related to tissue inflammation were not eliminated completely. Novel polymer-free drug delivery systems are now also being investigated in order to eliminate the use of polymers completely. This concept relies on the use of either non-polymeric biodegradable carriers for the drugs, or textured surfaces which act as drug reservoirs, or direct attachment of drugs on the surface by covalent bonding, crystallisation or chemical precipitation (Abizaid *et al.* 2010).

The YUKON® DES is the workhorse of polymer-free DES. It was part of the ISAR-TEST stent project and is one of the few commercially available polymer-free coronary

DESs in Europe. This design uses a 316LVM SS stent backbone whose surface is microtextured by means of grit-blasting. Sirolimus and Probucol are then loaded on the stent on-site, by means of a proprietary device which allows for tailored drug dosing (Garg *et al.* 2010, Wessely *et al.* 2005). SEM images of the surface of the stent before and after drug loading are shown in Figure 1. The adherence of the drug to the surface of the stent is enhanced by the inclusion of a low concentration (0.07%) of Shellac resin in the drug solution (Abizaid *et al.* 2010). Shellac is a natural, biocompatible resin which is used in a number of applications in the pharmaceutical and food industries.



**FIGURE 1 – SEM IMAGES OF THE SURFACE CHARACTERISTICS OF THE YUKON STENT BEFORE AND AFTER DRUG LOADING. (ABIZAID ET AL. 2010)**

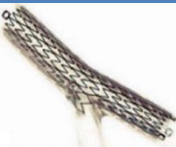
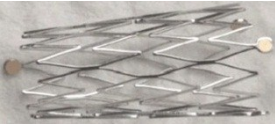

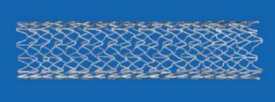

The results from the ISAR-TEST have proven non-inferiority of YUKON Sirolimus eluting stents when compared to permanent polymer Paclitaxel eluting stents (Garg *et al.* 2010). Furthermore, when the stent was used for dual drug delivery – Sirolimus and Probucol – it proved to have an efficacy comparable to permanent polymer Sirolimus or Zotarolimus eluting stents and low rates of ST even in large-scale studies (Byrne *et al.* 2009, Massberg *et al.* 2011). Release experiments have also shown that the system releases 70-80% of the drug over the first five days of immersion, followed by a slower release (www.translumina.de). It is questionable whether such a sustained release would be possible from a grit blasted surface without the use of the shellac resin. This raises questions on whether this stent is in reality a fully polymer-free DES or not, since shellac resin in essence is also a polymer, even though it is a naturally occurring one.

## 1.2 NITINOL STENTS

Nitinol has a number of advantages over conventional stent materials most of which derive from the material's superelasticity. Nitinol stents are self-expandable, and as such, do not require balloon deployment, resulting in less endothelial damage and lower crossing profile as well as more flexible stent delivery systems (Yoneyama *et*

*al.* 2009). Although a number of polymer-free DESs are commercially available, none of the ones for coronary applications employ Nitinol stent backbones. Recent developments in this area of research have shown that Nitinol stents gave favourable results due to their low strut thickness, flexibility and chronic outward force. Nitinol has also shown good biocompatibility, hemocompatibility and corrosion resistance when in simulated body environments (Shabalovskaya *et al.* 2008, Thierry *et al.* 2002). Furthermore, it can be seen that its characteristic material properties have encouraged its use in complex lesions (such as bifurcations, vulnerable plaques, peripheral vessels, small vessels or superficial vessels) for which conventional materials did not perform well (Yoneyama *et al.* 2009). This trend has been seen in both BMSs and DESs, with an increasing interest in Nitinol over the years. Some lacunae are, however, still present since Nitinol stents do not yet exist for all DES subsets. This is emphasized in Table 1 where we can observe that no Nitinol polymer-free DESs exist for coronary applications, while stents using polymeric drug carriers are available for a wide range of applications.

**TABLE 1 – OVERVIEW OF CURRENTLY AVAILABLE NITINOL DESs GROUPED ACCORDING TO APPLICATION.**

Stent	Drug	Drug carrier	Application	Status	Design
Stentys	Paclitaxel	Permanent Polymer	Coronary Bifurcations	CE	
Axxess Plus	Biolimus A9	Biodegradable Polymer	Coronary Bifurcations	CE	
Cardiomind Sparrow	Sirolimus	Biodegradable Polymer	Small vessels	Clinical trials	
Dynalink E	Everolimus	Permanent Polymer	Peripheral	Clinical trials	
ZilverPTX	Paclitaxel	Polymer-free	Peripheral	CE	

In addition to the effects of polymeric carriers, several researchers have suggested that the conventional anti-restenotic drugs used in DES are also the cause of delayed

re-endothelialisation (Puskas *et al.* 2009, Venkatraman *et al.* 2007). A quick evaluation of the main anti-restenotic drugs currently being used reveals that the drugs are either cytotoxic or cytostatic. Due to the fact that the effects of these drugs are not cell type specific, achieving the necessary reduction in vascular smooth muscle cell (VSMC) proliferation will also have deleterious effects on endothelial cell (EC) proliferation. This issue, although not free from controversies, has induced scientists to search for better drugs and bioactive agents which are able to inhibit VSMC proliferation while promoting endothelial healing.

6-Mercaptopurine (6-MP) (molecular structure shown in Figure 2) is one such drug which is currently being studied by our colleagues at the Amsterdam Medical Centre. In their studies, Pires *et al.* (2007) and Pols *et al.* (2010), have seen that local administration of 6-MP to hypercholesteremic transgenic mice resulted in increased protection against atherosclerosis development. Human VSMC proliferation was also inhibited during *in vitro* cell culture with 6-MP.

Their studies showed that 6-MP activates the nuclear receptor Nur77, both *in vitro* and in murine models, and inhibits neointima formation in the latter, without inducing vascular cell apoptosis. From their studies the authors conclude that this drug is able to down-regulate VSMC and monocyte proliferation, while up-regulating endothelial cell (EC) proliferation – an ideal behaviour for an anti-restenotic drug. They therefore propose this drug as a novel drug to be used for the prevention of in-stent restenosis (ISR).

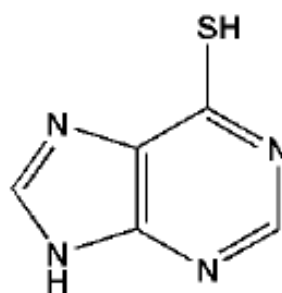


FIGURE 2 – MOLECULAR STRUCTURE OF 6-MP.

Currently available polymer-free drug eluting stents achieve drug retention and sustained release by employing:

- Non-polymeric, porous, biodegradable surface coatings – as in the VESTAsync stent,
- Microtextured surfaces – as in the Yukon and the BioFREEDOM stents,
- Direct attachment of the drug onto smooth or electropolished (EP) surfaces – as in the Amazonia PAX, the Zilver PTX and the OPTIMA stents (Abizaid 2010).

Microtextured and microporous surfaces have two main advantages over smooth surfaces which are:

- The surface features present give rise to a larger affective surface area for drug adsorption, therefore resulting in a higher reservoir capacity, and



- Rough surfaces were found to result in higher attachment and proliferation of endothelial cells (Shen et al. 2009).

The surface modification of Nitinol for stent applications has various aims, including:

- Improving the corrosion resistance of the material,
- Creating a barrier in order to limit nickel release,
- Improving the hemocompatibility and thromboresistance of the stent surface,
- Improving the compatibility of the material with vascular cells,
- Adding surface functionality to the material by creating a textured surface.

Recent studies have also investigated the development of porous NiTi surfaces by anodising. This is an electrochemical technique which is used in order to grow a layer of protective oxide at the surface of a passive metal. This is done by connecting the metal to be treated as the anode of an appropriate electrochemical cell within which it is suspended. The applied voltage is lower than the breakdown voltage of the oxide formed at the surface.

PEO is a surface modification technique, based on the anodic oxidation process, which operates at a voltage above the breakdown voltage of the oxide and therefore results in the occurrence of plasma micro-discharges along the surface immersed in the electrolyte. These micro-discharges result in the formation of microporosity, spread over the oxide layer formed. As the thickness of the oxide increases, so does the voltage; however, the number of discharges decreases, resulting in the formation of fewer, larger pores, thus resulting in higher surface roughness (Dong 2010). Curran and Clyne (2006) have seen that the porosity produced by this process is made up of both surface micropores as well as a large number of interconnected fine porosity. It is this mixture of pore sizes and their tortuous nanoporosity which makes these surfaces promising for drug loading and elution. The biocompatibility of Nitinol, with these surface modifications, is yet to be established.

The most important property of a controlled release drug delivery system is its ability to deliver the therapeutic dose of the drug at the required site and over a sufficient amount of time (Gultepe *et al.* 2010). The therapeutic dose and the required length of release are dependent on the specific anti-restenotic drug employed and on the state of the atherosclerotic plaque present in the treated vessel. This is why drug eluting stents are produced with a number of drug loads/release rates for the surgeons to choose from. Polymer-free drug eluting stents, which base their drug delivery system on an inorganic porous surface layer, use the size, distribution and density of the pores in order to vary the drug loads and the release kinetics. Fur-

thermore, the release kinetics are also effected by the tortuosity of the porosity, the surface free energy of the surface, the solubility of the drug and the size of the drug molecules (Siepman *et al.* 2012).

Due to the strong influence the porosity has on the drug loading capacity and the release kinetics, it is important to fully characterise the structure of the porosity present on the surface (Siepman *et al.* 2012). However, when the surface porosity is not interconnected with the substrate by a perpendicular path – as in the case of PEO treated surfaces – it is very difficult to quantify the porosity beyond what can be seen at the immediate surface. Nevertheless, the research by Curran and Clyne (2006) has shown that a large degree of fine, interconnected, tortuous porosity is present in PEO surfaces.

Tortuous porosity, however, also has a significant effect on the rate of diffusion through a porous structure. This is due to the fact that the distance travelled by the molecules is now no longer simply the perpendicular distance between the source (in our case the crystallised drug) and the surface of the sample but becomes more complex and may include changes in diffusion direction and dead ends.

### 1.3 AIM OF THE PROJECT

The aim of this project was to assess the potential of PEO treated Ni-Ti surfaces for the sustained release of the novel anti-restenitic drug 6-MP.

Nitinol coupons underwent PEO treatment in order to produce a microporous layer of titania at their surfaces. The oxidised surfaces were characterized for porosity, surface free energy and roughness. The drug was loaded by spraying multiple layers of an aqueous solution of 6-MP onto their surfaces. The release profiles of this drug were then measured by high-performance liquid chromatography (HPLC) in PBS solution at 37°C and compared to those obtained from electropolished surfaces. Finally, the experimental release kinetics achieved were fitted by means of two models used in literature for the simulation of drug release from polymer-free surfaces: Korsmeyer-Peppas model and a two-phase elution model based on Ficks' first law of diffusion.

This study was the first of its kind in the drug employed, in the chemistry of solvent used for the drug, in the drug application method for a fully-polymer-free system and in the surface modification which was applied to the Nitinol samples.

## 2. MATERIALS AND METHODS

---



## 2 MATERIALS AND METHODS

### 2.1 MATERIAL USED

The material used was a NiTi alloy, with 50.6 at. % nickel. It was provided in the form of a sheet 85mm wide by 300mm long and 1mm thick. The material was cut into strips 1cm wide and 85mm long and a hole was drilled into one end of the strips to enable the attachment of electrical connectors during electrochemical processing. The corners of the strips were rounded off by means of wet grinding with 320 grit abrasive papers. The strips were finally cleaned by ultrasonication for 10 minutes in isopropanol and deionised water, respectively, and stored in sterile sample bags before further processing.

### 2.2 SURFACE TREATMENT

The treatments conducted to modify the surfaces of the nitinol strips supplied were based on electropolishing (EP), which is the standard surface treatment for stents, and plasma electrolytic oxidation (PEO). Three types of samples were used in this study: EP, PEO treated and EP followed by PEO treatment (EP+PEO). The methodologies used for each of these treatments will be described in detail in the following sub-sections.

#### 2.2.1 ELECTROPOLISHING

Electropolishing (EP) was conducted in an electrolytic cell which consisted of a glass beaker with a volume of 120ml and a cylindrical stainless steel electrode which was of a smaller diameter than the beaker in order to allow its insertion within the latter. The cell was filled with 100ml of electrolyte which was a mixture of acetic acid ( $\text{CH}_3\text{COOH}$ ) and perchloric acid ( $\text{HClO}_4$ ) in the ratio 5:1 v/v, while stirring at 300 rpm by means of a magnetic stirrer (Ika, Netherlands). The Ni-Ti strips were then screwed to an insulated metallic rod and suspended in the centre of the electrochemical cell, allowing only 1cm of the strip length to be in contact with the electrolyte. The metallic rod and the cylindrical steel electrode (which was surrounding the Ni-Ti strip in the cell), were then electrically connected to a potentiostat so as to act as the anode and cathode of the electrolytic cell, respectively. The potentiostat was then set to 10 V and left to run for 7 minutes for each sample. At the end of the 7 minutes the potentiostat was switched off and the Ni-Ti strip was removed and flushed with running water for 10 minutes. The Ni-Ti strips were then briefly rinsed in deionised water, dried with compressed air and stored in clean sample bags for further processing. Each batch of electrolyte was used to polish a maximum of 5 samples, after which it was discarded and a new batch of electrolyte was prepared.

### **2.2.2 PLASMA ELECTROLYTIC OXIDATION**

Plasma electrolytic oxidation (PEO) was conducted in the same electrolytic cell used for electropolishing. The cell was filled with 100ml of frozen concentrated phosphoric acid ( $\text{H}_3\text{PO}_4$ ) as an electrolyte, while stirring at 300 rpm by means of a magnetic stirrer (Ika, Netherlands). The Ni-Ti strips were again screwed to an insulated metallic rod and suspended in the centre of the electrochemical cell, allowing only 1cm of the strip length to be in contact with the electrolyte. The metallic rod and the cylindrical steel counter electrode were then electrically connected to a galvanostat so as to act as the anode and cathode of the electrolytic cell, respectively. The galvanostat was then set to supply a current of 690mA (equivalent to  $30\text{A}/\text{dm}^2$  at the sample surface) and left to run until the voltage reached 55V. At this point, the galvanostat was switched off and the Ni-Ti strip was removed and flushed with running water for 10 minutes. The treated Ni-Ti strips were then briefly rinsed in deionised water, dried with compressed air and stored in clean sample bags for further processing. Each batch of electrolyte was used to treat a maximum of 4 samples, since after this amount of samples the temperature of the electrolyte would not be low enough to allow the treatment to proceed. The electrolyte was therefore refreshed and the used electrolyte was returned to the freezer, to be reused after a few hours of cooling.

## **2.3 SURFACE CHARACTERIZATION**

The surfaces of the as-received (AR), EP, PEO and EP+PEO samples were characterised by means of scanning electron microscopy (SEM), energy dispersive spectroscopy (EDS), surface profilometry and drop shape analysis (DSA). Furthermore, SEM images of the PEO and EP+PEO samples were used in order to characterise the surface porosity present on this type of samples. The methodologies used will be described in detail in the following sub-sections.

### **2.3.1 SCANNING ELECTRON MICROSCOPY AND ENERGY DISPERSIVE SPECTROSCOPY**

The surfaces of the AR, EP, PEO, and EP+PEO samples were examined by scanning electron microscopy (SEM, JSM-6500F, JEOL) using an accelerating voltage of 5 kV. Before imaging, the samples that had undergone PEO (ie the PEO and EP+PEO samples) were sputter coated with carbon to enhance their conductivity. The elemental composition was estimated on the surface by means of an energy dispersive X-ray spectrometer (EDS, INCA Energy, Oxford Instruments) coupled with the SEM equipment.

The samples were first observed and photographed at various magnifications in the range of 50 to 10,000 times and elemental analysis was carried out at the latter magnification. Imaging and EDS analysis were performed at three different locations on the supplied samples in order to have a good overview of how the surface morphology of the samples varies and to be able to estimate the average composition of the treated surfaces.

### 2.3.2 SURFACE POROSITY CHARACTERIZATION

The surface porosity present on PEO and EP+PEO samples was characterised by analysing the images obtained by SEM by means of an image analysis software such as Adobe Photoshop CS6. Three samples of each set were used and three images were taken at random spots on each sample, at 5,000 times magnification. The images were loaded into the image analysis software and the scale of the image was set according to the scale bar present in the image. A special selection tool (the “magic wand” tool) was then used in order to select all the open pores present on the surface of the material. The software was then able to automatically calculate the size and surface area of each pore and generated a report. The data in this report was then used in order to calculate:

- The degree of porosity (i.e. the fraction of the total surface area made up by pores),

$$Porosity = \frac{A_{pores}}{A_{total}} \dots (1)$$

- The pore density (i.e. the number of pores present per centimetre squared),

$$Pore\ Density = \frac{Number\ of\ Pores}{Area} \dots (2)$$

- The average pore size (i.e. the average pore diameter),
- The average pore area.

The results obtained were then used in order to compare the type of porosity obtained when different types of surface treatment protocols were applied to the Ni-Ti samples.

### 2.3.3 SURFACE PROFILOMETRY – ROUGHNESS MEASUREMENT

Surface profilometry was used in order to measure the roughness present on AR, EP, PEO and EP+PEO samples. Three samples were used for each type of surface finish and five repetitions of the measurements were conducted on each sample. The samples were placed on a flat surface and their roughness was measured by means of a Surtronic 3+ surface roughness tester. Prior to measurement, samples were stuck to

the testing table by means of double sided adhesive tape, ensuring that they were well attached to the tape in order to avoid any motion of the samples during testing. All the parameters measured by the device were recorded and their average values and standard deviations were calculated for each sample subset.

#### 2.3.4 DROP SHAPE ANALYSIS

In order to calculate the surface free energy of AS, EP, PEO, and EP+PEO Nitinol samples, it was necessary to first measure the contact angles between these materials and water as well as diiodomethane. The samples were cleaned by ultrasonication for 5 minutes in 70% ethanol and deionised water, respectively. The samples were then dried by means of compressed air and placed in open, sterile sample bags, not allowing the bag to touch the surface of the samples which needed to be tested.

The instrument which was used to measure the contact angle was a Kruss Drop Analyser 100. The software of the machine was set to perform dynamic measurement thus taking 48 measurements of the contact angle in 48 seconds while the machine ejected 10µl of HPLC grade water onto the surface of the material and performed in triplicate. This process was repeated with diiodomethane for all samples in order to enable the calculation of the surface free energy.

The standard values for the polar and dispersive components of the surface tension of the two liquids used are listed in Table 2. The surface free energy was calculated according to Fowke's theory.

**TABLE 2 – STANDARD VALUES FOR POLAR AND DISPERSIVE COMPONENTS OF LIQUIDS USED.**

Liquid	Overall Surface Tension (mN/m)	Dispersive Component (mN/m)	Polar Component (mN/m)
Diiodomethane	50.8	50.8	0.0
Water	72.8	26.4	46.4

The surface energies were calculated by means of the following formula:

$$\sigma_s = \sigma_s^D + \sigma_s^P \dots (3)$$

The dispersive component of the surface energy of the solid can be calculated from:



$$\sigma_S^D = \frac{\sigma_{LDi}(\cos \theta_{Di} + 1)^2}{4} \dots (4)$$

Since the diiodomethane has only dispersive components, the  $\sigma_{LDi}$  = 50.8 and the contact angle is the one measured using this liquid.

The polar component can then be calculated by using the data for the water as well as  $\sigma_S^D$  by using:

$$\sigma_S^P = \left( \frac{\left( \frac{\sigma_{Lw}(\cos \theta_w + 1)}{2} \right) - (\sigma_{Lw}^D \cdot \sigma_S^D)^{0.5}}{\sigma_{Lw}^P^{0.5}} \right)^2 \dots (5)$$

## 2.4 DRUG LOADING AND RELEASE

This section will deal with the methods used in order to evaluate the reservoir capacity and the ability to maintain a sustained release of 6-MP of PEO treated surfaces.

### 2.4.1 DRUG LOADING

#### 2.4.1.1 6-MP SOLUTION PREPARATION

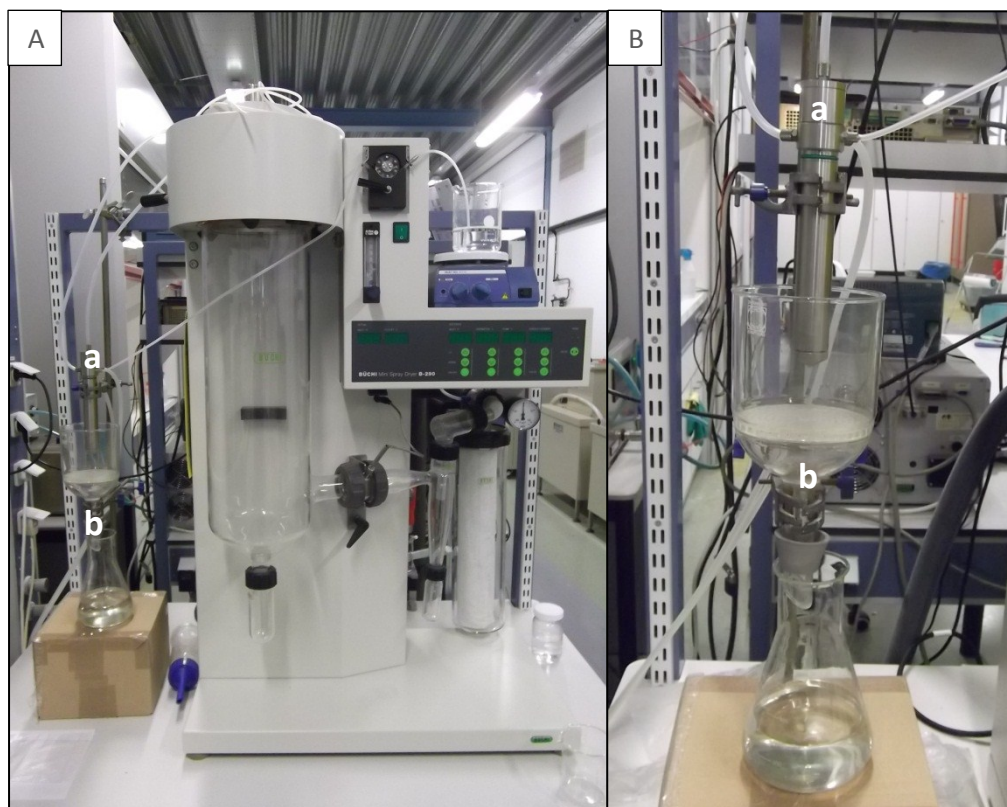
250ml of 1.25mg/ml 6-MP stock solution were produced by following the ensuing procedure: 313.7 mg of 98% 6-mercaptopurine monohydrate were weighed and dissolved in 25ml of 0.1M NaOH solution. The solution was stirred by means of a magnetic stirrer until all the drug had dissolved. The remaining 225ml of deionised water were then added to the solution and stirring was continued for a further 10 minutes in order to ensure the solution was homogeneous. This solution was used for drug loading as required. In order to limit the effects of drug degradation, the solution was discarded every 12 hours and a new batch of the solution was prepared.

#### 2.4.1.2 DRUG LOADING – SPRAYING

The samples to be loaded by spraying were first ultrasonicated for 10 minutes in 70% ethanol and deionised water respectively. The samples were then dried in compressed air and placed on absorbent tissue.

The configuration of a BUCHI B-290 Spray dryer was modified in order to enable drug spraying as seen in Figure 3. The device was connected to an external spray nozzle (a) and a drip catch (b) with a perforated glass plate was clamped under the nozzle in

order to act as a sample holder while allowing excess drug solution to drain and be collected in a flat bottomed flask.



**FIGURE 3 – SET-UP USED FOR DRUG SPRAYING. (A) FULL VIEW, (B) CLOSE-UP OF SPRAYING NOZZLE.**

The drip catch was fixed at a distance of 3.8cm from the nozzle. This distance was chosen as it minimised the interaction of the drip catch walls with the spray cone, while maximizing the area on the glass plate which was being wet homogenously by the spray cone at the chosen gas flow rates. During drug spraying, the samples were placed within the latter mentioned area, keeping the same position for each spray cycle, in order to limit inter-sample variability.

The 6-MP stock solution described previously was used as the spraying solution. This solution was placed in a beaker, stirred at 200rpm by means of a magnetic stirrer and fed to the peristaltic pump. The nitrogen flow rate was set to 138L/hr or 192L/hr and the peristaltic pump was switched on at 2% performance (equivalent to 29mL/hr) and left to run for 10 seconds per spray cycle. The drug coated sample was then removed from within the drip catch by means of long tweezers, placed on absorbent paper and left to dry under a warm blower in a fume cabinet for a couple of minutes. The process was repeated as necessary in order to achieve a wide range of drug loads on the surfaces under investigation. After the final drying step the samples were briefly rinsed in one of the following release media and dried again:

- 100% deionised water
- 50% deionised water, 50% ethanol
- 70% deionised water, 30% ethanol

A separate series of samples was loaded by immersion, the most used method in literature. Therefore the ultrasonicated and dried samples were immersed in a beaker containing the 6-MP stock solution, taking care that the samples did not overlap and were at a distance from one another. The beaker was then placed in an ultrasonic bath for 10 minutes in order to aid the infiltration of the solution into the porosity present on the surface of the PEO treated samples, followed by a further 50 minutes of plain immersion. After this period of time, the samples were removed vertically by means of tweezers and left to dry in a fume cabinet.

#### **2.4.1.3 DRUG LOAD DETERMINATION**

---

In order to determine the amount of drug loaded onto the surfaces of the samples, the loaded samples were immersed in amber bottles containing 8ml of deionised water and 2ml of 0.1M HCl to limit drug degradation. These bottles were then ultrasonicated for 3 hours, shaken vigorously, left to shake in an immersion bath at 37°C for 21 hours, and again shaken vigorously. Samples of 1ml were extracted from the bottles, placed in capped 1.5ml eppendorf tubes and stored at -18°C to avoid drug degradation before drug content evaluation by HPLC analysis. Three samples were used for each sample set in order to enable the calculation of the average drug load and standard deviation. Drug loading efficiency was calculated as the percentage of 6-MP still present on the surface after rinsing of drug coated samples.

#### **2.4.2 DRUG RELEASE**

The drug release experiments started with a preliminary study which looked at the release of 6-MP from EP+PEO samples which were loaded either by immersion, or by spraying 6 layers at 138L/hr gas flow followed by water rinsing, or by spraying 6 layers at 192L/hr gas flow followed by water rinsing. This study was necessary to identify the limitations present in our system and helped in the development of a final protocol which was then used in all successive studies.

##### **2.4.2.1 PRELIMINARY PROTOCOL**

---

Initially the samples were immersed in amber glass bottles containing 5 ml of Phosphate Buffered Saline (PBS) in a stationary incubator at 37°C. At each sampling time point, the bottles were shaken gently and a 1ml sample of the release medium was extracted and replaced with fresh PBS. The samples were placed in capped 1.5ml

eppendorf tubes and stored at -18°C to avoid drug degradation before drug content evaluation by HPLC analysis.

#### **2.4.2.2      PROTOCOL FOR RELEASE IN PBS**

---

The drug coated samples were immersed in amber glass bottles containing 10 ml of Phosphate Buffered Saline (PBS) in a stationary incubator at 37°C. At each sampling time point, the bottles were shaken gently and the NiTi samples were removed by means of tweezers and placed in the caps of the bottles. The bottles were shaken once again, a 0.5ml sample of the release medium was extracted and the NiTi samples were placed back into the bottle. The samples extracted were placed in capped 1.5 ml eppendorf tubes together with 0.5ml of deionised water and stored at -18°C to avoid the occurrence of drug degradation before drug content evaluation by HPLC analysis.

#### **2.4.2.3      PROTOCOL FOR RELEASE IN HIGHLY ACIDIFIED PBS**

---

The drug coated samples were now immersed in amber glass bottles holding 10 ml of Phosphate Buffered Saline (PBS) containing 25mM HCl in an incubator at 37°C, under shaking conditions. At each sampling time point, the bottles were shaken gently and the NiTi samples were removed by means of tweezers and placed in the caps of the bottles. The bottles were shaken once again, a 0.5ml sample of the release medium was extracted and the NiTi samples were placed back into the bottle. The samples extracted were placed in capped 1.5 ml eppendorf tubes together with 0.5ml of deionised water and stored at -18°C to avoid the occurrence of drug degradation before drug content evaluation by HPLC analysis.

### **2.4.3 DRUG STABILITY**

The stability of 10µg/ml 6-MP was studied in:

- PBS
- 100mM NaOH
- Deionised water
- PBS containing 0.09mM NaOH
- PBS containing 0.09mM NaOH and 0.9mM HCl
- PBS containing 0.9M HCl
- PBS containing 25mM HCl
- 25mM HCl

This was done by dissolving 100µg/ml of 6-MP in PBS, NaOH or deionised water as necessary and then diluting this further with appropriate amounts of PBS, 0.1M

NaOH and 0.1M HCl to obtain the variants described above. These solutions were then placed in amber glass bottles and left in an incubator at 37°C. Samples of 1ml were extracted at regular intervals, placed in capped 1.5ml eppendorf tubes, and stored at -18°C to avoid the occurrence of further drug degradation before drug content evaluation by HPLC analysis.

#### **2.4.4 HIGH PERFORMANCE LIQUID CHROMATOGRAPHY (HPLC)**

HPLC is a high pressure chromatographic technique used to separate, quantify and identify the different types of molecules present in a solution. It uses a pressurised liquid (eluent) to transport the sample to be analysed through separating column. This column is filled with particles which delay the transport of certain molecules while letting through other molecules more easily, thus achieving separation. The UV absorbance of the exiting fluid is then used in order to calculate the concentration of a particular molecule present in the sample. Each molecule has a characteristic UV absorbance wavelength and a characteristic time at which it exits the column (retention time). It is therefore possible to identify which molecule each peak of absorbance belongs to and quantify the concentration of such a molecule by calculating the area of the related peak.

##### **2.4.4.1 PREPARATION OF STANDARD MIXTURES**

---

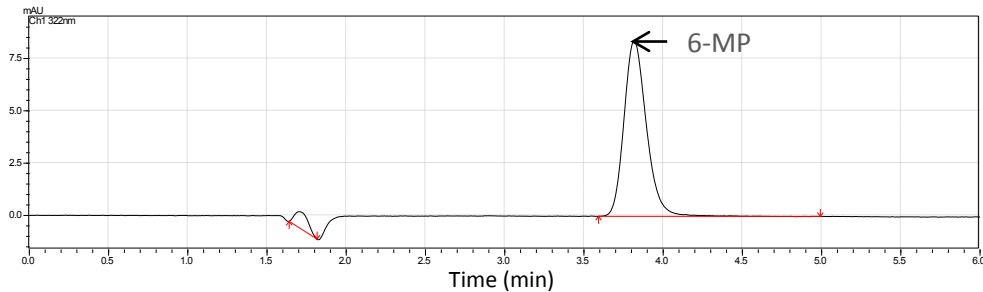
A stock solution of 6-MP at a concentration of 200µg/ml was prepared by dissolving the appropriate amount of 6-mercaptopurine mononhydrate (98%) in 1ml of 0.1M NaOH, diluting with 22ml of deionised water and acidifying with 2ml of 0.1M HCl. The stock solution was then used to produce five standard mixtures containing 0.1 µg/ml, 0.5 µg/ml, 1 µg/ml, 5 µg/ml and 10 µg/ml of 6-MP, by diluting with deionised water as appropriate. Aliquots of 1ml of these standard mixtures were placed in capped 1.5ml eppendorf tubes and stored at -18°C to avoid the occurrence of drug degradation before HPLC analysis.

##### **2.4.4.2 HPLC ANALYSIS**

---

The 6-MP content of standard mixtures and experimental samples was determined by means of a Varian Prostar HPLC equipped with a mobile phase delivery system and a Chromospheres C18 reversed-phase column (150 x 4.6mm, 5µm particle size). The concentration of 6-MP present in each sample was determined using a Varian Prostar spectrometer reading at 322 nm, with a retention time of 3.8 minutes. The eluent used was a mixture of 7.5: 92.5 (v/v) methanol – water containing 100mM triethylamine and adjusted to pH 3.2 by means of concentrated phosphoric acid. The eluent was filtered and pumped through the machine at a flow rate of 1ml/min, activating the pump at least 30 minutes before the start of the analysis to ensure the

system had been adequately purged from any contaminants. The machine was calibrated every day of use by analysing vials containing the five standard mixtures described earlier and a vial containing deionised water. A typical HPLC chromatogram for 6-MP is illustrated in Figure 4.



**FIGURE 4 – TYPICAL HPLC CHROMATOGRAM FOR 6-MP.**

## 2.5 MATHEMATICAL MODELLING OF DRUG ELUTION

In order to better characterise the release kinetics observed for EP+PEO samples, the data obtained was fitted by means of two models used in literature for the simulation of drug release from polymer-free surfaces: Korsmeyer-Peppas model (Moseke 2012) and a two-phase elution model based on Ficks' first law of diffusion (Peng 2009). The fit of these models to the experimental data was evaluated by calculating the Pearson product moment correlation coefficient ( $r$ ) which tends to 1 with increasing correlation.

The Korsmeyer-Peppas model is a power law in the form of:

$$\frac{M(t)}{M_{\infty}} = kt^n \quad \dots (6)$$

where  $M(t)$  is the accumulated released mass at time  $t$ ,  $M_{\infty}$  is the total amount of drug loaded on the surface which would be released at  $t \rightarrow \infty$ ,  $k$  is the kinetic constant and  $n$  is the release exponent (Moseke 2012). In thin films, when  $n \leq 0.5$ , the release of the drug is diffusion based.

In this model  $M_{\infty}$  can be measured experimentally and  $k$  and  $n$  can be extrapolated from the experimental data. If logs to base e are taken on both sides of equation 4 we get:

$$\ln \frac{M(t)}{M_{\infty}} = \ln k + n \ln t \quad \dots (7)$$

Therefore, by applying the natural logarithm to the experimental data and fitting a straight line to this data it is possible to obtain  $n$  and  $k$ .

Due to the fact that the data obtained experimentally exhibited a two-phase release behaviour, a two-phase release model was also used to approximate the release kinetics observed. In this model the release is assumed to be based on a fast release phase and a slow release phase, both of which are based on first-order release kinetics. Assuming that the two release phases are independent from each other, the two-phase model therefore has the form:

$$M(t) = M_{\infty} - M_f \cdot e^{-C_f t} - M_s \cdot e^{-C_s t} \quad \dots (8)$$

where  $M(t)$  is the accumulated released mass at time  $t$ ,  $M_{\infty}$  is the total amount of drug loaded on the surface which would be released at  $t \rightarrow \infty$ ,  $M_s$  is the mass available for slow release,  $M_f$  is the mass available for fast release, and  $C_s$  and  $C_f$  are the first-order kinetic constants for slow and fast release, respectively (Peng 2009).

Furthermore it is known that  $M_{\infty} = M_f + M_s$ ; therefore by identifying the transition between fast and slow release it is possible to determine  $M_f$  and  $M_s$ . Moreover,  $C_s$  and  $C_f$  can be calculated from the experimental data by considering the first and the last few data points obtained in the experimental data.





## 3. RESULTS AND DISCUSSION

---

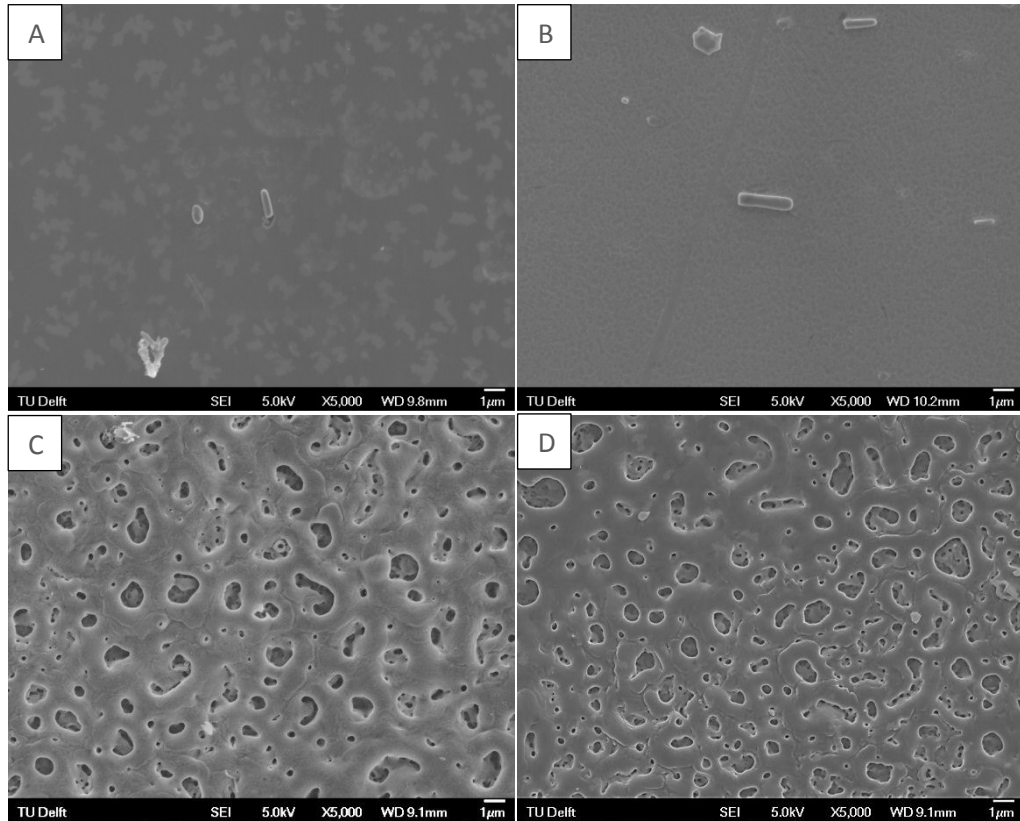


### 3 RESULTS AND DISCUSSION

#### 3.1 SURFACE CHARACTERIZATION

##### 3.1.1 SEM AND EDS ANALYSIS

The surface morphologies of AR, EP, PEO treated and EP+PEO treated samples obtained by SEM can be seen in Figure 5.



**FIGURE 5 – SEM IMAGES (5000x) OF SURFACE MORPHOLOGIES OF NiTi SAMPLES (A) AS-RECEIVED, (B) ELECTROPOLISHED, (C) PEO TREATED, (D) ELECTROPOLISHED AND PEO TREATED**

In Figure 5 A and B it can be seen that the surfaces of the as-received and electropolished samples are rather smooth with some inclusions visible at the surface. These inclusions however, do not remain visible when such samples undergo PEO treatment, as seen in Figure 5 C and D respectively. In the latter images it can also be seen that, as expected, the PEO treatment gave rise to the formation of porosity in the surface of the samples. The pores produced vary in size between a couple of microns to a couple of tenths of a micron in diameter and larger pores are connected to finer porosity within them, that extends deeper into the titania layer. Also, when comparing Figure 5 C to Figure 5 D one may see that the EP pre-treatment gave rise to some changes in the type of porosity obtained during PEO. A more thorough characterization of the porosities obtained and a further discussion

of the differences present between these two types of PEO treated samples will be given later in the next subsection.

The elemental composition of the surfaces of AR, EP, PEO treated and EP+PEO treated samples was analysed by means of EDS. The results obtained were tabulated and presented in Table 3.

**TABLE 3 – MEAN ELEMENTAL COMPOSITIONS OBTAINED BY EDS ANALYSIS**

Sample	Atom (% $\pm$ SD)				Ni/Ti ( $\pm$ SD)
	Ni	Ti	O	P	
AR	44.42 $\pm$ 3.49	51.22 $\pm$ 0.60	4.37 $\pm$ 3.27	–	0.87 $\pm$ 0.07
EP	49.65 $\pm$ 0.27	50.35 $\pm$ 0.27	–	–	0.99 $\pm$ 0.01
PEO	10.05 $\pm$ 1.05	17.45 $\pm$ 0.97	53.71 $\pm$ 2.28	18.79 $\pm$ 1.39	0.57 $\pm$ 0.08
EP+PEO	9.03 $\pm$ 0.13	18.55 $\pm$ 1.40	52.58 $\pm$ 0.97	19.84 $\pm$ 0.54	0.49 $\pm$ 0.03

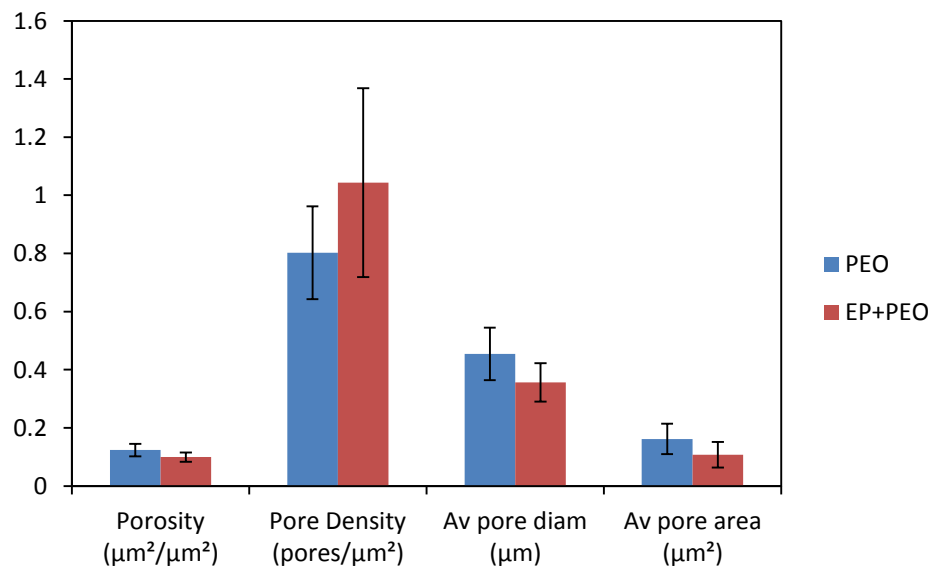
From these results one can conclude that electropolishing is effective at removing the native oxide present on the surface of the metal and exposes the underlying metal which is more homogenous. This can also be seen from the fact that the standard deviation of the values obtained for the EP samples is significantly lower than that obtained for the AR samples.

Once the material undergoes PEO treatment the surface composition changes significantly. This is due to the formation of a layer of oxide on the surface and the uptake of phosphorus from the electrolyte. Moreover, since titanium is more reactive than nickel, it oxidises in preference to it, thus causing a decrease in the ratio of nickel to titanium. Another interesting thing one may observe in these results is that, when PEO is preceded by electropolishing, we once again see a decrease in the standard deviation of the elemental compositions, confirming that electropolishing is effective at homogenising the surface both from a morphological and from a chemical perspective.

### 3.1.2 SURFACE POROSITY CHARACTERIZATION

As described previously, SEM images of the PEO and EP+PEO samples were used in order to characterise the surface porosity present. From the analysis conducted it was possible to calculate the porosity, pore density, average pore diameter and average pore area for the two types of surfaces. The results obtained are illustrated in Figure 6, where the bar shows average value calculated for each set and the error bars represent the standard deviations in each set. As can be clearly seen, there were no significant differences between the two surfaces studied however the general trend observed was that the electropolishing pre-treatment resulted the formation of an increased number of pores which were smaller in diameter. Moreover, the average porosity falls from 12.4% to 9.9% when electropolishing is employed be-

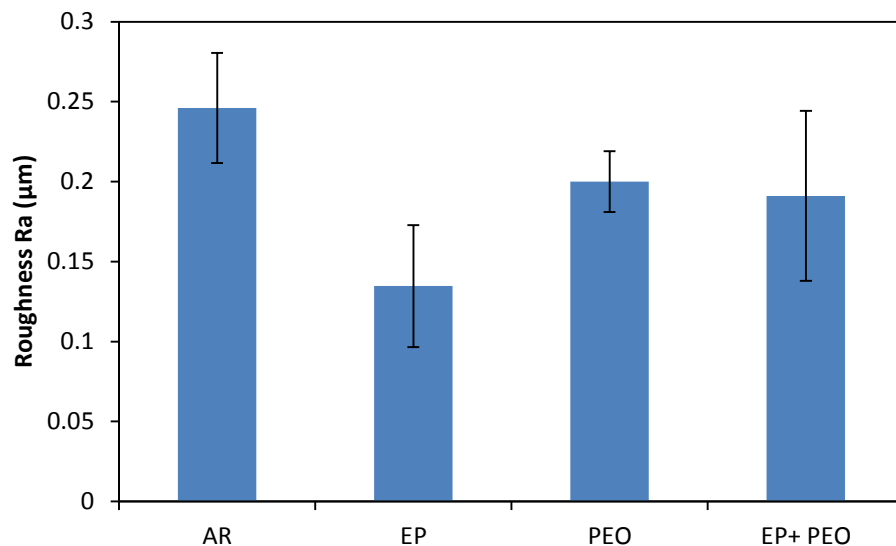
fore PEO treatment. In order to see whether significant differences do exist between the two groups it might therefore be useful to image a larger number of samples in order to be able to narrow down the standard deviation.



**FIGURE 6 – POROSITY CHARACTERISTICS FOR PEO AND EP+PEO SAMPLES, ERROR BARS REPRESENTING THE STANDARD DEVIATION OF EACH VALUE.**

### 3.1.3 ROUGHNESS MEASUREMENT

The average Ra values obtained for the four sample sets tested, and their standard deviations were plotted in Figure 7.



**FIGURE 7 – MEAN RA MEASUREMENTS FOR AS-RECEIVED (AR), ELECTROPOLISHED (EP), PLASMA ELECTROLYTIC OXIDATION TREATED (PEO), AND ELECTROPOLISHED AND PEO TREATED (EP+PEO) SAMPLES. ERROR BARS REPRESENT THE STANDARD DEVIATION FROM THE MEAN VALUE IN THE SAMPLE SET TESTED.**

Here we can observe that electropolishing significantly decreases the Ra value of the surface, as expected. Furthermore, it can also be observed that conducting PEO on the untreated NiTi results in a surface roughness which is higher than in the case of electropolishing but which is not significantly different from the untreated material. On the other hand, when we consider the samples which were first EP and then PEO treated we see that the average roughness has increased after PEO treatment but there was a large spread of results, resulting in no significant differences between EP and EP+PEO Ra values. Another interesting observation is that the mean Ra values of the two sets of samples which underwent PEO were found to be only marginally different. This suggests that during PEO, oxide growth at the surface results in a canceling of micrometric features present on the surface prior to treatment, such as surface roughness.

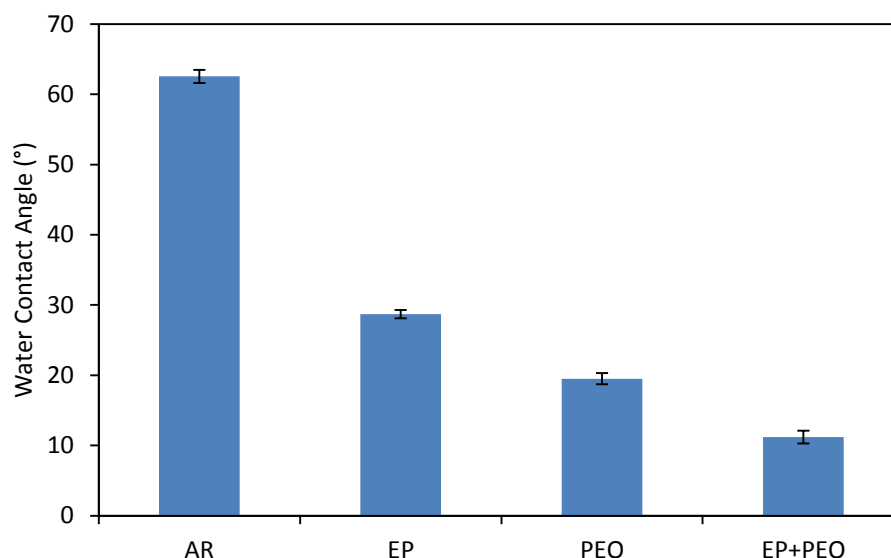
### 3.1.4 DROP SHAPE ANALYSIS

The average contact angles and surface energies were calculated for each material from the average contact angles measured by the software on the samples and they were tabulated in Table 4.

**TABLE 4 – MEASURED WATER AND DIODOMETHANE CONTACT ANGLES AND CALCULATED SURFACE FREE ENERGY FOR THE FOUR SURFACES TESTED.**

Sample	Water Contact Angle (°)	Diiodomethane Contact Angle (°)	Surface Energy (mJ/m <sup>2</sup> )
AR	62.55 ± 0.93	37.37 ± 0.19	49.81 ± 0.34
EP	28.71 ± 0.59	41.19 ± 2.04	67.29 ± 1.12
PEO	19.51 ± 0.79	31.56 ± 0.45	72.74 ± 0.37
EP+PEO	11.21 ± 0.91	35.32 ± 1.34	74.41 ± 0.40

In order to aid in the visualisation of the differences present between the four types of surfaces analysed, the water contact angle data was plotted in Figure 8. Here it can be seen without doubt that the surface treatment history of the samples resulted in significant changes in the properties of the surface. In our case, a decrease in water contact angle is beneficial since it points towards better cell compatibility and spreading once the stents are implanted. Furthermore, since the drug spraying solution is water based, a lower water contact angle results in better spreading of the drug on the surface and possibly also better infiltration of the drug within the surface porosity present on EP+PEO surfaces. It is however surprising that the contact angle on EP+PEO surfaces is significantly lower than that for PEO when none of the other characteristics measured for these two surfaces showed any significant differences. The other characteristics did however show a higher standard deviation for EP+PEO surfaces, leading us to think that it was this variability on the micro-scale which led to such a difference in contact angle. These results justify the use of EP+PEO treatment as opposed to PEO treatment only and have led to the use of EP+PEO treated samples for further studies in drug elution.



**FIGURE 8 – WATER CONTACT ANGLE AVERAGE VALUES FOR AR, EP, PEO AND EP+PEO SAMPLES. ERROR BARS REPRESENT THE STANDARD DEVIATION OF THE AVERAGE VALUES MEASURED.**

## 3.2 6-MP LOADING AND RELEASE

### 3.2.1 6-MP SOLUBILITY

The solubility of 6-MP in various solvents as found in literature are summarised in Table 5. The best solvents for 6-MP were found to be NaOH, DMSO and DMF. Due to spraying equipment available, only aqueous solutions of 6-MP could be used. Unfortunately it was also found that although sodium hydroxide (NaOH) solutions are the only aqueous solutions to provide a good solubility at room temperature, they also give rise to a significant amount of drug degradation. It was therefore decided to opt for a weak NaOH solution in order to limit drug degradation and allow for in-house drug spraying.

**TABLE 5 – SOLUBILITY OF 6-MP IN VARIOUS SOLVENTS**

Solvent	Temperature (°C)	Solubility (mg/ml)	Reference
Water	23	0.1700	Waranis 1987
	30	6.8480	pubchem
	100	9.5836	pubchem
Alkali Solutions	Soluble with slow decomposition		pubchem
<b>1M NaOH</b>		50.0000	Sigma Aldrich
Ethanol	20	0.8300	pubchem
<b>DMSO</b>	23±1	34.8000	Waranis 1987
		Soluble but methylates it	Kroeplin 1998
<b>DMF</b>	23±1	14.5000	Waranis 1987
Oleic Acid	23±1	0.0030	Waranis 1987
Isopropyl myristate	23±1	0.0034	Waranis 1987
1-Octanol	23±1	0.2300	Waranis 1987
Propylene Glycol	23±1	6.2000	Waranis 1987
Ethylene Glycol	23±1	3.0000	Waranis 1987
Formamide	23±1	9.1000	Waranis 1987

One of the most successful polymer-free drug eluting stents developed to date is the Yukon stent, in which Sirolimus is sprayed on to the surface of a microporous stent surface on site. However, in most of the research on polymer-free drug elution, the drugs are loaded onto the surfaces being studied by simple immersion or, in some cases, pipetting. Nevertheless, spraying enables a better control of drug loading and distribution compared to immersion deposition and provides advantages in the application to stents and in the standardization of the procedure. During the spraying procedure, it is possible to change the characteristics of the spray cone by modifying the gas flow rate, the drug solution flow rate, and the distance of the sample from the spray nozzle.

### 3.2.2 EFFECT OF SPRAYING CONDITIONS ON 6-MP LOADS AND SURFACE DISTRIBUTION

#### 3.2.2.1 INFLUENCE OF GAS SPRAY FLOW ON 6-MP LOADS

In this preliminary study, the samples were loaded by spraying 6 layers at two different gas spray flows: 138L/hr or 192L/hr. In between sprayed layers, the samples were left to dry naturally in a fume cabinet and after the final drying step they were briefly rinsed in 50% ethanol solution and once again left to dry naturally. The results of 6-MP release after 6 hours of immersion (preliminary protocol) are illustrated in Figure 9 and were used as a preliminary indication of the amount of drug loaded under the different conditions. However, it may not be excluded that these values might show only the burst release of the drug. For comparison, samples loaded by immersion for one hour were included in this experiment.

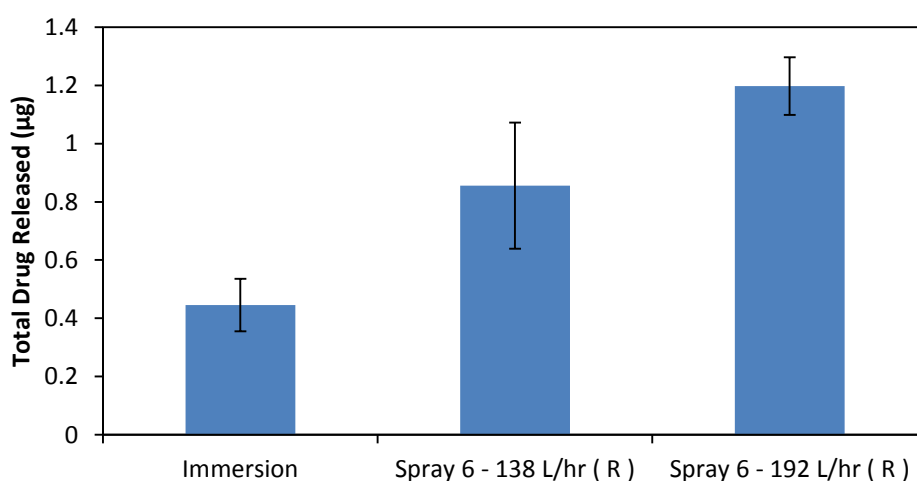


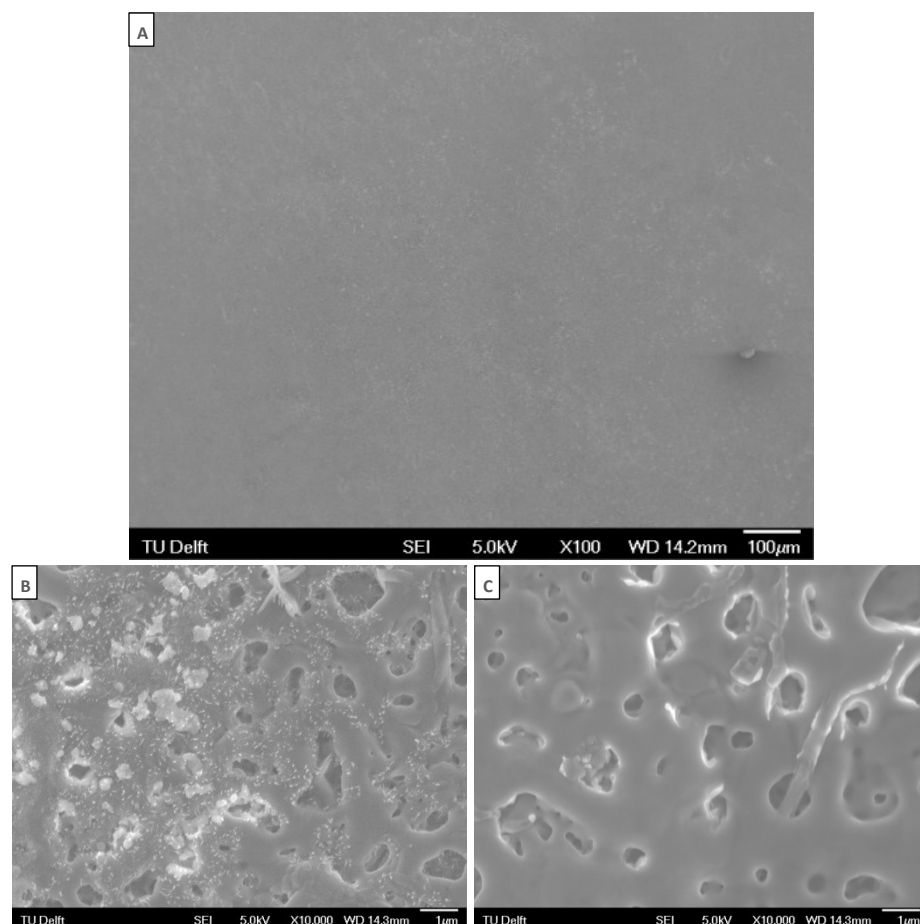
FIGURE 9 – TOTAL 6-MP RELEASE IN PBS AT 37°C AFTER 6 HOURS FROM EP+PEO SAMPLES LOADED BY IMMERSION AND DRUG SPRAYING AT 138L/HR AND 192L/HR GAS FLOW.



The results illustrated in Figure 9 suggest that it was possible to achieve significantly higher drug loads by spraying than by immersion, and the highest drug load was obtained in the samples sprayed at the high flow rate. The gas flow rate has a strong influence on the properties of the spray cone formed. Increasing the flow rate results in a wider cone as well as the formation of smaller droplets which travel at a higher speed since more energy is available for fluid dispersion. Therefore, the 6-MP solution droplets sprayed at higher flow hit the surface of the samples with more energy. The drug solution can therefore penetrate deeper into the porosity, allowing these surfaces to retain more of the applied drug after rinsing. To increase the amount of 6-MP loaded on the surfaces, an increased number of layers was sprayed at the high flow and the surface distribution of the drug was examined by SEM.

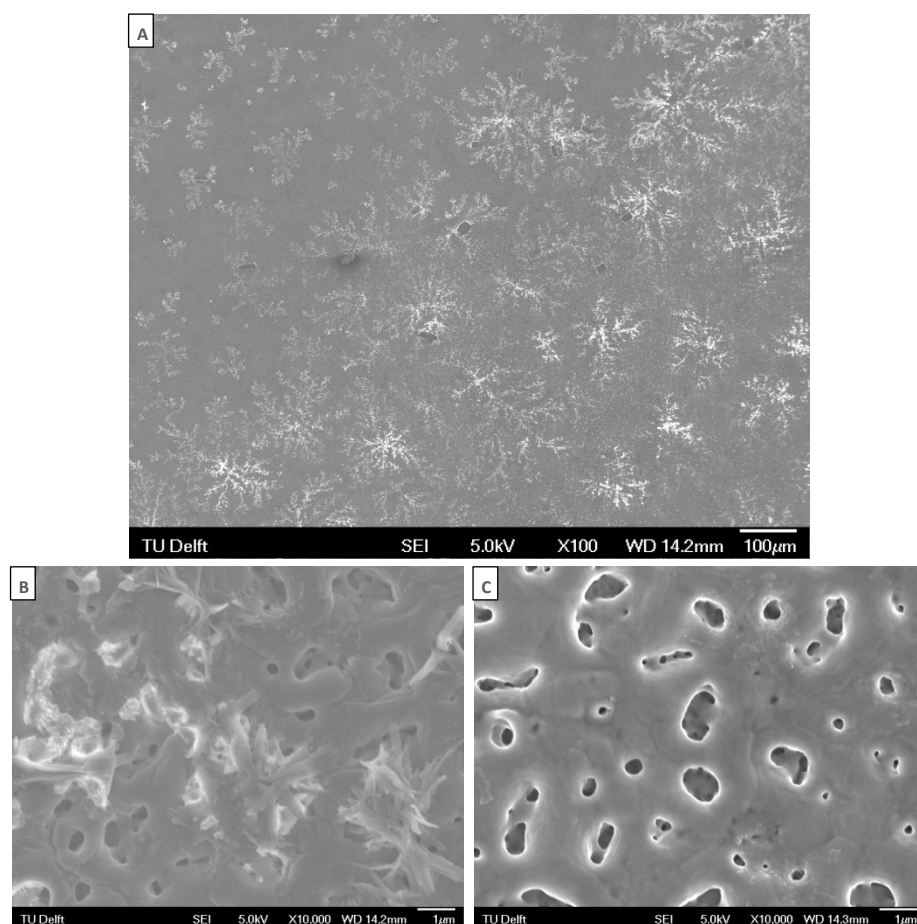
### 3.2.2.2 INFLUENCE OF NUMBER OF SPRAYED LAYERS ON 6-MP DISTRIBUTION

Figure 10 to Figure 12 show the results obtained after spraying 6, 10 and 20 layers of drug respectively at 192l/hr, followed by rinsing in 50% ethanol.



**FIGURE 10 – SEM IMAGES OF THE SURFACE OF EP+PEO SAMPLES AFTER SPRAYING 6 LAYERS OF 6-MP SOLUTION AT 192 L/HR AND RINSING IN 50% ETHANOL. (A) 100X MAG, (B) 10,000X MAG AT THE CENTRE OF THE SAMPLE, AND (C) 10,000X MAG AT THE EDGE OF THE SAMPLE.**

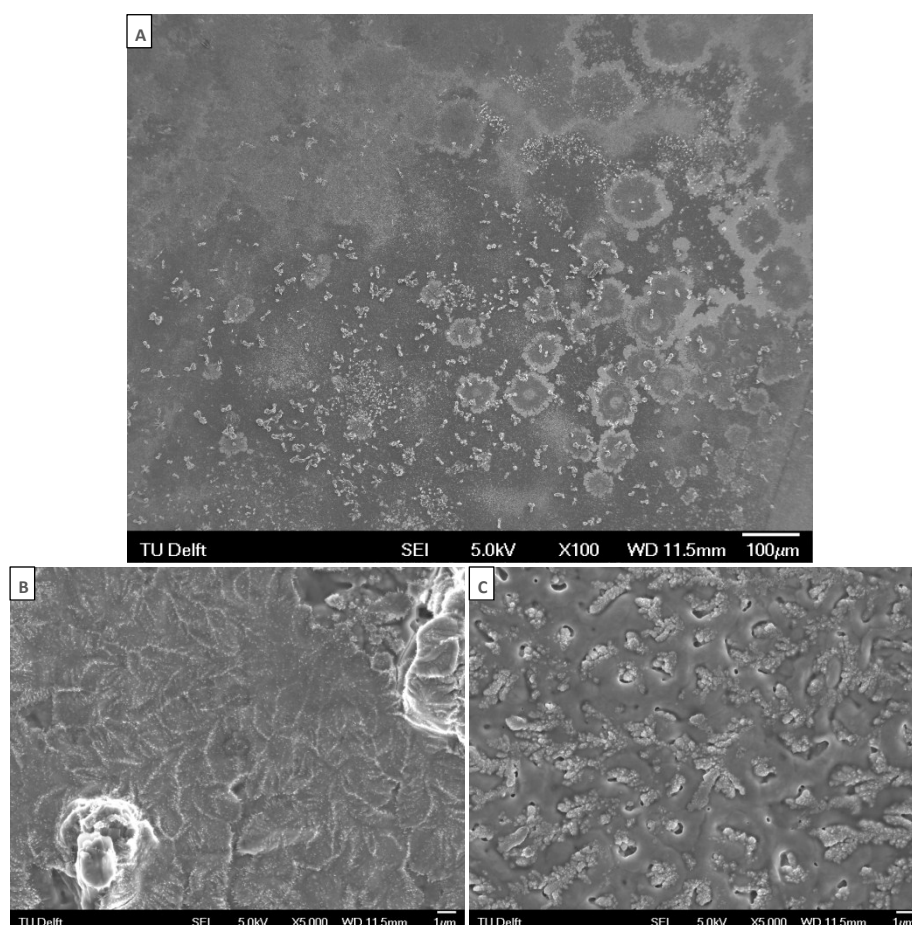
After spraying six layers (Figure 10) it is seen that although at a low magnification (A) there appear to be no large localised accumulations of drug; higher magnifications reveal that the drug is not distributed homogeneously over the surface. It was seen that a larger amount of drug was present at the centre of the sample (B) than at the edge (C). It was hypothesised that this might be caused during the drying process. Since the samples tend to dry from the edge inwards, the drug has a tendency to move with the solvent till it reaches the solubility limit and deposits on the surface. It is however also possible to see that most of the drug still present after rinsing tends to crystallise within the porosity. Unfortunately, since the size of the crystals present were relatively small it was not possible to confirm the nature of the different types of crystals seen in Figure 10 B by EDS.



**FIGURE 11 – SEM IMAGES OF THE SURFACE OF EP+PEO SAMPLES AFTER SPRAYING 10 LAYERS OF 6-MP SOLUTION AT 192 L/HR AND RINSING IN 50% ETHANOL. (A) 100X MAG, (B) 10,000X MAG AT THE CENTRE OF THE SAMPLE, AND (C) 10,000X MAG AT THE EDGE OF THE SAMPLE.**

When the number of sprayed layers is increased from six to ten (Figure 11) it is seen that although the size of the crystals grows (Figure 11 A and B) there is still inhomogeneity in the distribution of the drug on the surface, leaving areas close to the edges of the samples (Figure 11C) with very few visible crystals. This, on the other hand,

does not rule out the formation of a drug monolayer but it is highly improbable that such a monolayer would be sufficient to reach the desired drug loads.



**FIGURE 12 – SEM IMAGES OF THE SURFACE OF EP+PEO SAMPLES AFTER SPRAYING 20 LAYERS OF 6-MP SOLUTION AT 192 L/HR AND RINSING IN 50% ETHANOL. (A) 100X MAG, (B) 5,000X MAG AT THE CENTRE OF THE SAMPLE, AND (C) 5,000X MAG AT THE EDGE OF THE SAMPLE.**

The images shown in Figure 12 suggest that much more 6-MP is loaded onto the surface after spraying 20 layers. Although some inhomogeneity in drug distribution still exists (Figure 12 A) with a thick layer of the drug forming in some areas of the surface (Figure 12 B), an almost ideal distribution of the drug within the pores obtained in other areas (Figure 12 C). These results therefore suggest that an ideal drug distribution may be obtained by further optimizing the final rinsing step.

Furthermore, it was confirmed that such crystals were 6-MP by means of EDS analysis (typical spectrum obtained shown in Figure 13). From this spectrum it can be seen that the area analysed contains nickel, titanium, oxygen and phosphorus, similarly to what was seen for the uncoated EP+PEO samples in Table 3. Furthermore, sodium and sulphur were also found on the drug coated samples. The sodium detected de-

rived from the NaOH used in the stock solution of 6-MP while the sulphur derived from the 6-MP itself.

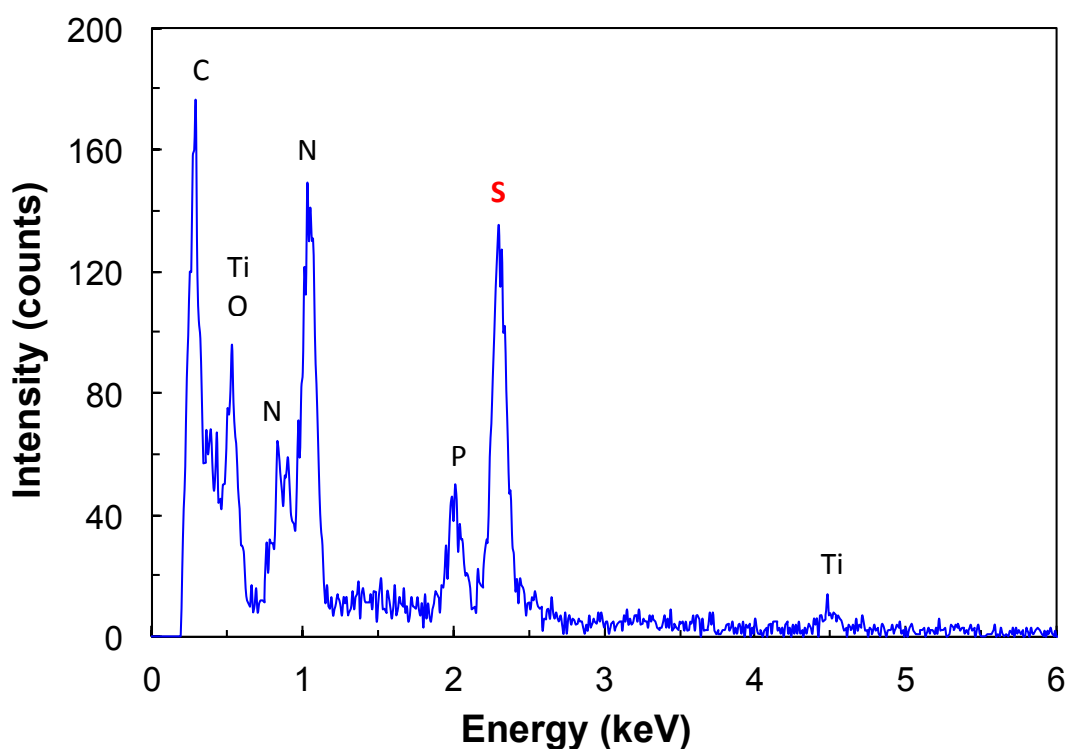


FIGURE 13 – EDS SPECTRUM OBTAINED FROM CRYSTALS FORMED ON THE SURFACE OF EP+PEO SAMPLES AFTER SPRAYING 20 LAYERS OF 6-MP AT 192 L/HR AND RINSING IN 50% ETHANOL.

### 3.2.2.3 INFLUENCE OF RINSING MEDIUM ON DRUG DISTRIBUTION AND LOADS

Having seen that the 50% ethanol solution did not yield ideal rinsing conditions, alternative rinsing media, namely deionised water and 30% ethanol solution, were investigated.

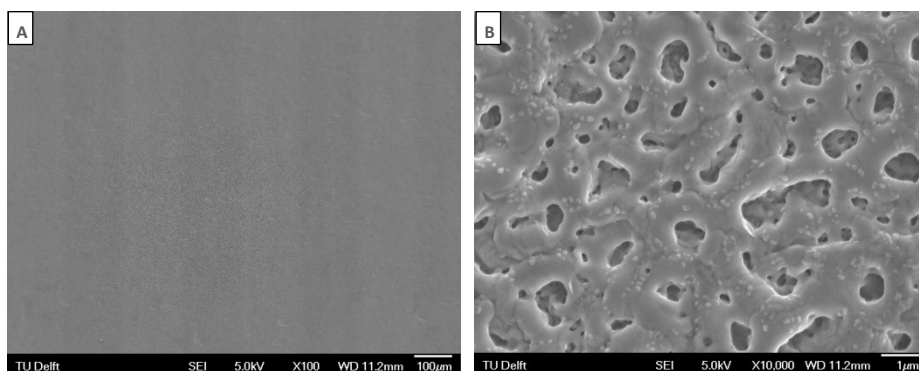
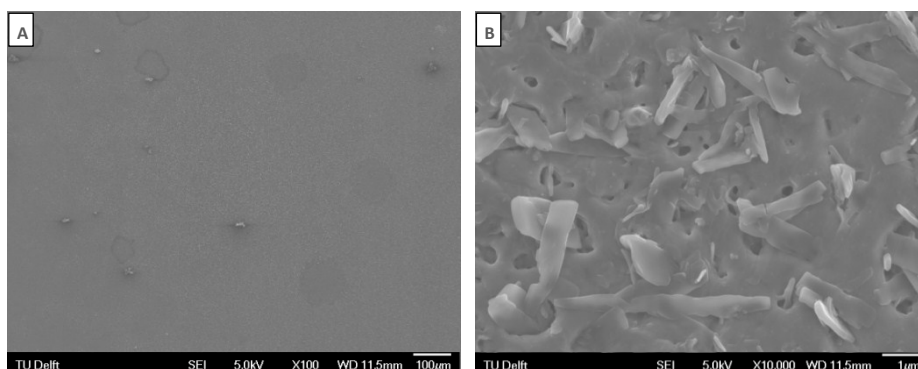


FIGURE 14 – SEM IMAGES OF THE SURFACE OF EP+PEO SAMPLES AFTER SPRAYING 20 LAYERS OF 6-MP SOLUTION AT 192 L/HR AND RINSING IN WATER: (A) 100x MAG, (B) 10,000x MAG.

Some trials with deionised water as the rinsing medium (Figure 14) showed that this removed a large proportion of the deposited drug. The rinsing step was now able to eliminate the large crystals seen previously at low magnifications and only left small crystals of the drug scattered over the surface (Figure 14B). This rinsing medium was therefore deemed inadequate and it was decided to investigate a rinsing medium with an intermediate ethanol content.

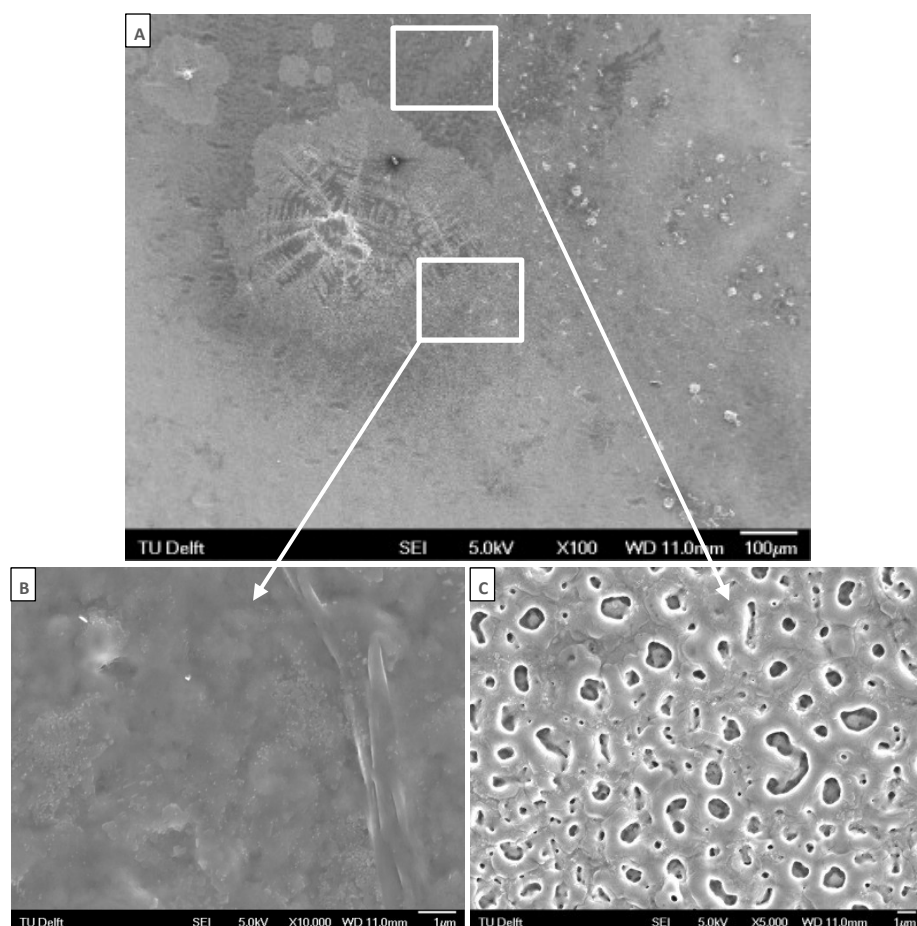


**FIGURE 15 – SEM IMAGES OF THE SURFACE OF EP+PEO SAMPLES AFTER SPRAYING 20 LAYERS OF 6-MP SOLUTION AT 192 L/HR AND RINSING IN 30% ETHANOL: (A) 100x MAG, (B) 10,000x MAG.**

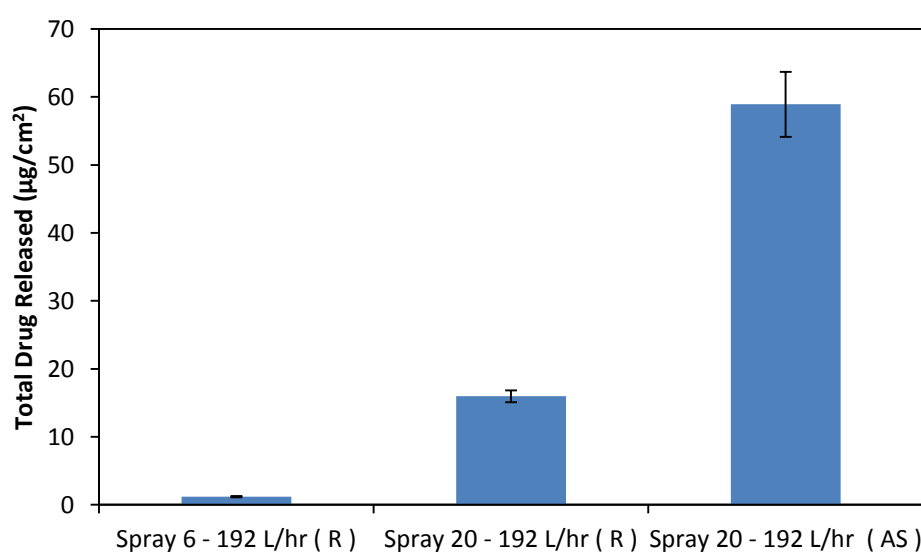
When we compare the results obtained after 30% ethanol rinsing (Figure 15A) with those for 50% ethanol rinsing (Figure 12A), a significant improvement in the homogeneity of the drug distribution is seen. Furthermore, when 30% ethanol rinsing is employed the sample is covered in a monolayer of the drug, with drug crystals extending outwards from within the pores present on the surface, as seen in Figure 15B. The nature of the crystals seen in Figure 15B and of the drug layer covering the entire surface was analysed by means of EDS, yielding a spectrum similar to that shown in Figure 13. The latter revealed the presence of sulphur in both sites thus confirming that 6-MP was present since this was the only possible source of sulphur.

For comparison, the SEM images obtained for as-sprayed Spray 20 samples are shown in Figure 16. The images shown highlight the importance of including a rinsing step in order to remove large accumulations of drug from the surface like the one shown in Figure 16 A. Most of the surface of the sample is covered in a thick layer of drug like the one shown in Figure 16 B and only a small region at the edge has the lower drug cover shown in Figure 16 C. It is therefore important to include a rinsing step in order to limit the amount of drug released during the burst phase. The effect of the rinsing step on drug loading was assessed further by comparing the 6-MP released after 6 hours of immersion from the as-sprayed to that from the rinsed (30% ethanol) Spray 20 samples in Figure 17. Data on the amount of drug released from the rinsed (50% ethanol) Spray 6 samples was included as a reference.





**FIGURE 16 – SEM IMAGES OF THE SURFACE OF EP+PEO SAMPLES AFTER SPRAYING 20 LAYERS OF 6-MP SOLUTION AT 192 L/HR. (A) 100X MAG, (B) 10,000X MAG AT THE CENTRE OF THE SAMPLE, AND (C) 5,000X MAG AT THE EDGE OF THE SAMPLE.**



**FIGURE 17 – TOTAL DRUG RELEASED AFTER 6 HOURS OF IMMERSION IN PBS AT 37°C FOR RINSED(R) SPRAY 6 (50% ETHANOL) AND SPRAY 20 (30% ETHANOL) SAMPLES COMPARED TO AS-SPRAYED (AS) SPRAY 20 SAMPLES.**

Upon analysis of Figure 17 one immediately notices that the amount of drug retained at the surface of the samples after rinsing is not directly proportional to the number of layers of drug which were deposited. It seems that when a larger number of layers were employed, the drug penetrates deeper into the porosity and was therefore not immediately washed away during rinsing. Furthermore, the Spray 20 samples had been rinsed with 30% ethanol which was seen by SEM to remove more drug than the 50% ethanol used to rinse the spray 6 samples. On the other hand we also see that rinsing removes a large amount of the drug sprayed onto the surface and therefore a large portion of the sprayed drug had not yet penetrated into the porosity.

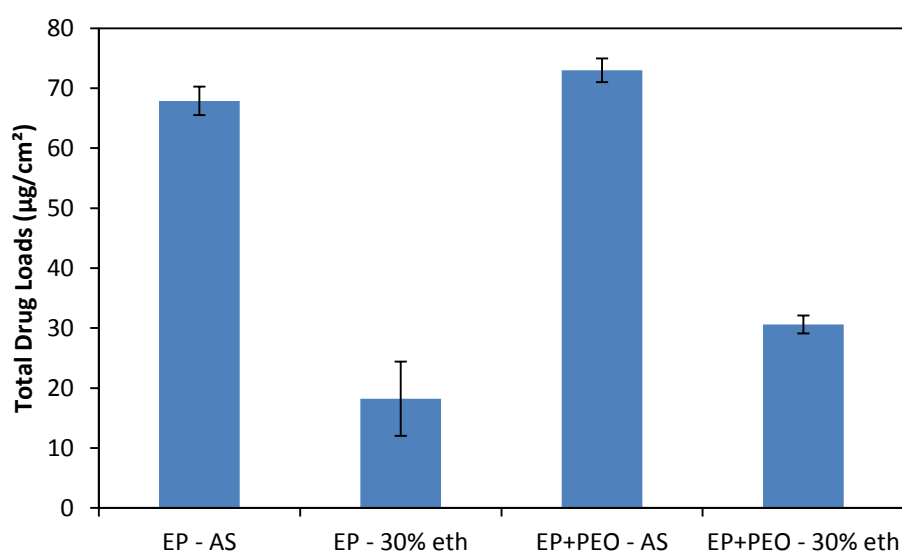
Drying and rinsing steps should therefore be optimised further in order to allow loading of more drug on these surfaces. It may be beneficial to include brief intermediate rinsing steps during the spraying cycle in order to avoid the formation of large accumulations of drug at the surface. . Furthermore, drying may be conducted within a vacuum furnace to enhance the drug penetration while speeding up the drying process in order to avoid the formation of large crystals. In addition, other methods of drug application, such as simple immersion and pipetting, should be further investigated. In this work only a short study was made on the use of immersion at the beginning of the project; however, the time of immersion was only 1 hour, which is in contrast with the 24-72 hours found in literature (Aw *et al.* 2011 & 2012, Gulati *et al.* 2012, Losic *et al.* 2011). Longer immersion times would allow the drug to penetrate deeper into the porosity therefore achieving higher drug loads and longer periods of sustained release. Moreover, the drug solution used was the same one used for spraying therefore containing only 1.1mg/ml of 6-MP and using NaOH as a solvent. Future studies should thus also consider the use of organic solvents in this case for the reasons mentioned previously

Based on these preliminary findings, the release studies that followed focused on samples which were coated with 20 layers of 6-MP solution by spraying at a flow of 192 L/hr and either left as-sprayed or rinsed in 30% ethanol.

### **3.2.3 EFFECT OF PEO TREATMENT ON DRUG LOADING**

The only Nitinol, polymer-free drug eluting stent currently available on the market is the Zilver PTX (designed for peripheral vessels). The final surface of this stent is EP and is loaded with Paclitaxel without the use of any binders or polymers. The differences in drug loading potential of EP and EP+PEO treated samples were therefore studied and the results obtained are presented in Figure 18. The drug loads were determined according to the protocol described under section 2.4.1.3.

The study on drug loads confirmed that the EP+PEO surfaces are able to retain a significantly higher amount of drug during spraying. During drying the drug has a tendency to slide off the smooth EP surfaces. On the other hand, the porosity present on EP+PEO surfaces allows such samples to retain more of the sprayed drug solution, therefore resulting in higher final drug loads. The drug load remains higher for EP+PEO samples even after rinsing due to their higher reservoir capacity. This is confirmed by calculating the drug loading efficiency of the two surfaces, where it is seen that, while EP surfaces have a drug loading efficiency of 26.8%, EP+ PEO surfaces exhibit an efficiency of 41.9%.



**FIGURE 18 – MEAN DRUG LOADS PRESENT ON SPRAY 20 EP AND EP+PEO SAMPLES, WITH OR WITHOUT RINSING IN 30% ETHANOL (N≥4). ERROR BARS REPRESENT THE STANDARD DEVIATION FROM THE MEAN.**

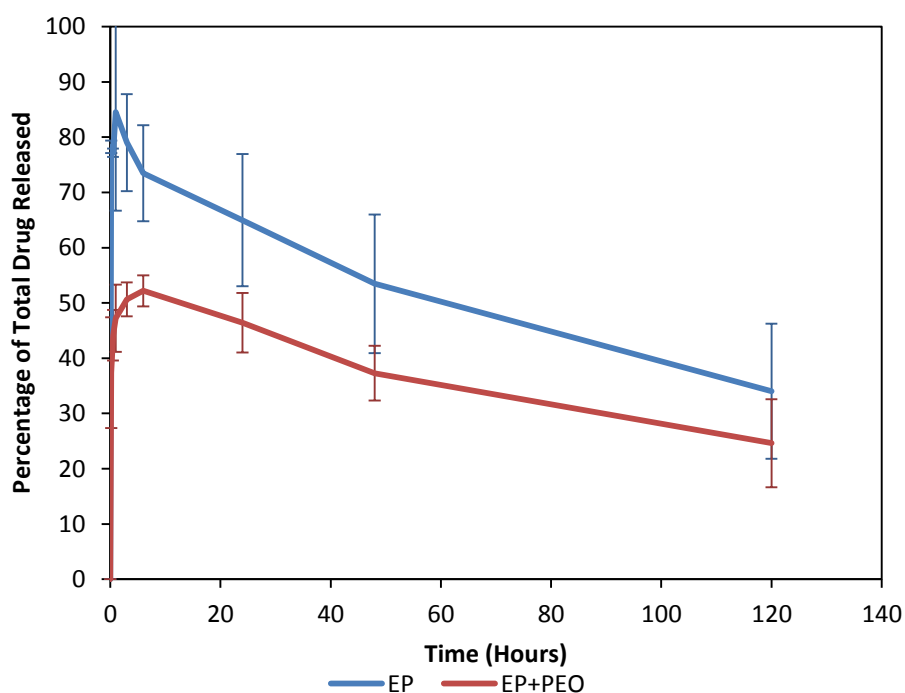
However, the drug loads obtained on rinsed EP+PEO surface are well below the desired  $100\mu\text{g}/\text{cm}^2$  (Garg 2010). In order to enable higher drug loads to be incorporated in such surfaces it is necessary to make the most of the available porosity. From current observations during the spraying procedure it was seen that increasing the number of layers might not give significant improvements since beyond 20 layers the number and size of large crystals forming on the surface increases. Ways of making use of the deeper porosity must therefore be sought. Employment of organic solvents (for the drug spraying solution) with lower surface contact angles on EP+PEO samples, and higher 6-MP solubility might give the desired results. Other options include varying the loading conditions in terms of the drying and rinsing steps, as mentioned previously.



On the other hand, the desired loading of this novel drug has yet to be established based on the *in vitro* and *in vivo* response of VSMCs and ECs, thus not ruling out the fact that the loads obtained may already be enough for this system. It was therefore decided to move on with the current system since the aim of this project was to assess the ability of such surfaces to sustain the release of 6-MP and not to assess their ability to reach the aforementioned drug load.

### 3.2.4 IN VITRO RELEASE PROFILES

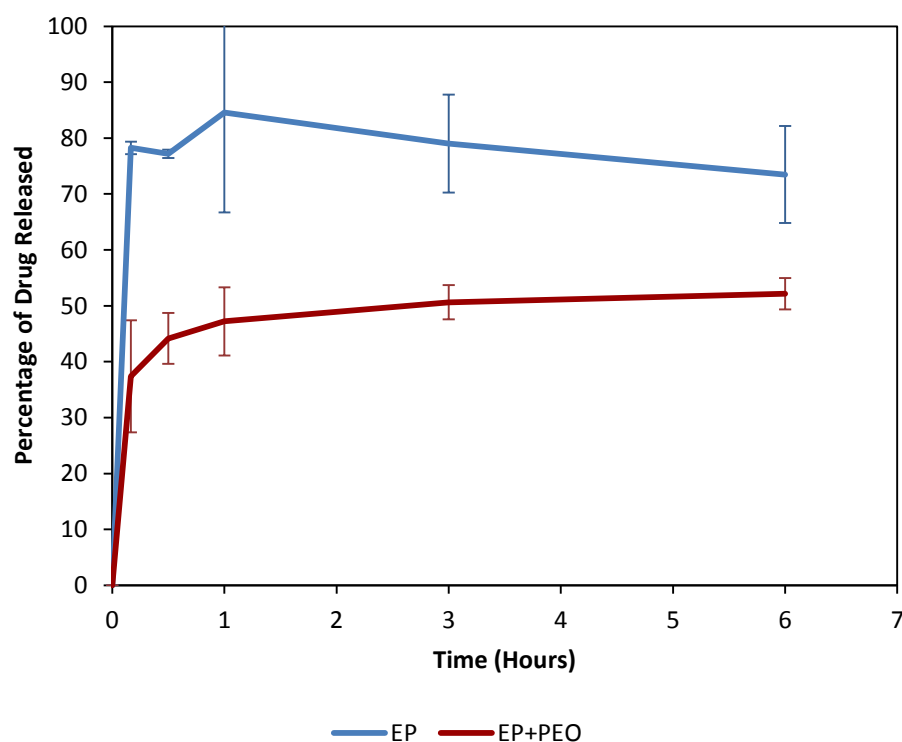
The release of 6-MP in PBS at 37° in static conditions from EP and EP+PEO samples which were loaded by spraying 20 layers of 6-MP solution at a gas flow rate of 192L/hr, followed by brief rinsing in 30% ethanol was studied and the results obtained are illustrated in Figure 19.



**FIGURE 19 – 6-MP RELEASE IN PBS AT 37°C DURING THE FIRST 120 HOURS FROM EP+PEO SAMPLES LOADED BY DRUG SPRAYING 20 LAYERS AT 192L/HR, WITH 30% ETHANOL RINSING.**

A striking feature of the data presented in Figure 19 is that the concentration of 6-MP in the samples analysed by HPLC decreased over time, resulting in a decrease in the calculated percentage of total amount of drug released. It was hypothesised that this might be due to the NaOH still present on the surface from the drug spraying solution. Although it was known that the drug was unstable in alkaline solutions, it was not expected that the NaOH would have such a strong influence on the degradation of the drug during release, especially after the rinsing step. Other factors which

might have had an influence on the drug stability were the PBS itself and the stationary conditions employed for release.



**FIGURE 20 – 6-MP RELEASE IN PBS AT 37°C DURING THE FIRST 6 HOURS FROM EP+PEO SAMPLES LOADED BY DRUG SPRAYING 20 LAYERS AT 192L/HR, WITH 30% ETHANOL RINSING.**

Upon closer analysis of the release profile of 6-MP during the first 6 hours of immersion (Figure 20) it can be seen that while the EP samples show a sharp burst ( $\approx 78\%$ ) of drug within the first 10 minutes of immersion, the EP+PEO samples release only half as much ( $\approx 37\%$ ) within the same time period. Furthermore, EP+PEO samples continue releasing the drug gradually over the first 6 hours of immersion. If it were possible to stop the degradation altogether, the EP+PEO surface is expected to show a sustained release of 6-MP over a much longer period of time. These findings indicate that EP+PEO surfaces do not only provide a higher reservoir capacity for loading of 6-MP, but also show potential for sustained release of this drug relative to EP surfaces.

### 3.2.5 DRUG STABILITY

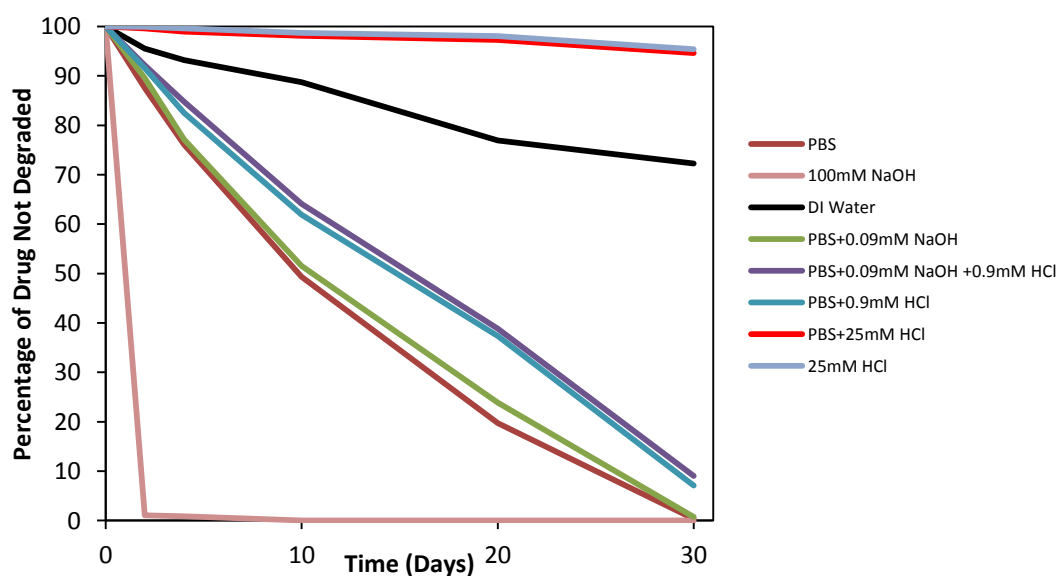
It was decided to study in more detail the stability of 6-MP in various media including NaOH and PBS, in order to better understand which components influence the drug stability and to be able to formulate a release medium which would stop such a fast

degradation from occurring, thus allowing the study of PEO-treated surfaces as drug carriers, independent of drug stability. The rationale behind each of the media studied is outlined in Table 6. Each solution had an initial concentration of 10µg/ml of 6-MP and was studied over a period of 30 days.

**TABLE 6 – SOLUTIONS EMPLOYED FOR THE STUDY OF 6-MP STABILITY**

Solution	pH	Comments
PBS	7.4	Simulated body fluid
0.1M NaOH	13.0	Solvent (Negative control)
Deionised water	7.0	Blank
PBS + 0.09mM NaOH	7.4	Model environment to study the effect of solvent on drug stability
PBS + 0.09mM NaOH +0.9mM HCl	7.2	
PBS + 0.9mM HCl	7.2	
PBS + 25mM HCl	2.2	Highly acidified PBS
25mM HCl	1.98	High stability medium (Positive control)

The results obtained are shown in Figure 21. The concentrations of NaOH and HCl chosen for the second, third and fourth medium were based on the calculation that in order to reach the 100µg/cm<sup>2</sup> of 6-MP which was being aimed for, a maximum of 0.09mM NaOH should be released during the release experiments, assuming that the same ratio of 6-MP to NaOH present in the spraying solution, is kept on the drug coated surface. Different concentrations of HCl were used in order to study the effect of NaOH neutralisation on drug stability.



**FIGURE 21 – DEGRADATION OF 6-MP AT 37°C IN VARIOUS RELEASE MEDIA, OVER A 30 DAY PERIOD.**

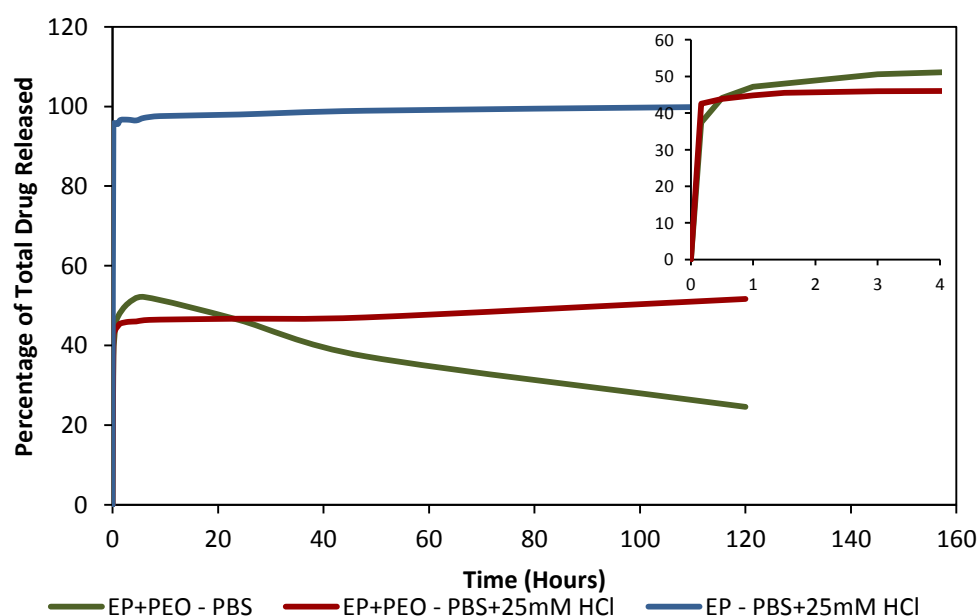
The data presented in Figure 21 shows that the main cause of 6-MP degradation during the previous release experiment may be attributed to PBS itself and not to the total increase in alkalinity brought about by the NaOH, since when this was added to PBS no significant change in the rate of degradation was observed. The contribution

of PBS to the degradation of 6-MP can be confirmed by comparing the rate of degradation in the latter to the one observed in deionised water, which was much lower. Moreover, it can be seen that slight acidification (0.9mM of HCl) of PBS was found to be effective at reducing the rate of degradation of 6-MP. The percentage of degraded 6-MP therefore fell from about 50% to about 35% over a 10-day period. Such a rate of degradation is however still too high and additional acidification is necessary in order to reduce this further.

The role of acidification in the stability of 6-MP was confirmed by the data shown for the degradation of 6-MP in 25mM HCl and PBS containing 25mM HCl. These modified release media resulted in an insignificant amount of degradation over the period of study. Although they are not relevant to the intended biomedical application of such surfaces, at this stage of the research the acidified PBS medium was used for further release experiments. This enabled us to study EP+PEO surfaces as drug carriers, independent of drug degradation.

### 3.2.6 EFFECT OF MODIFIED CONDITIONS ON *IN VITRO* RELEASE

The release profiles obtained from EP+PEO surfaces in the modified media over a 5 day period were compared to the profile obtained in PBS in Figure 22. The results obtained from EP samples in acidified PBS, loaded under the same conditions, were included as a reference.

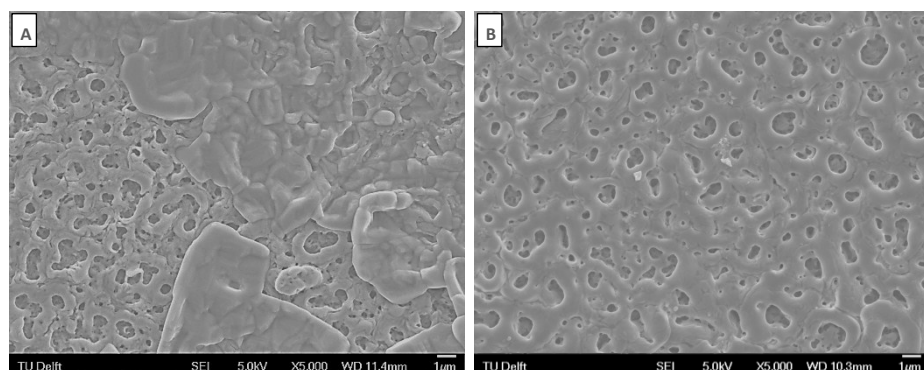


**FIGURE 22 – 6-MP RELEASE IN PBS AND PBS + 25mM HCl AT 37°C DURING THE FIRST 120 HOURS OF IMMERSION FROM EP AND EP+PEO SAMPLES LOADED BY DRUG SPRAYING 20 LAYERS AT A GAS FLOW RATE OF 192L/HR WITH 30% ETHANOL FINAL RINSING. INSERT SHOWING ENLARGED INITIAL 10 HOUR PORTION.**

Analysis of Figure 22 immediately reveals the efficacy of medium acidification in suppressing 6-MP degradation. Furthermore the release profile of EP+PEO surfaces in this medium shows two distinct phases: a burst phase in the first 10 minutes when about 42% of the drug is released at an average rate of 1.3 $\mu$ g/min, followed by a slow release thereafter at an average rate of 0.0153 $\mu$ g/min. At the end of the 5 day period the total percentage of drug released was 52%. In contrast, EP samples released most ( $\approx$ 95%) of the loaded drug within the first 10 minutes of immersion. This highlights the superiority of PEO treated surfaces over EP treated surfaces in sustaining the release of 6-MP. This superiority is derived from the micropores produced during PEO treatment which act as drug reservoirs, away from the immediate surface of the material. The drug must therefore first dissolve and then diffuse through the porosity in order to be released to the surrounding medium, making the solubility of the drug a determining parameter for the rate of release.

The advantages of the EP+PEO surfaces studied are highlighted further when we compare the release kinetics obtained with those for the Zilver PTX and the Yukon found in literature. The Zilver PTX releases 98% of the Paclitaxel within 24 hours (*in vivo*) (FDA executive report) while the Yukon stent releases 70-80% of the Sirolimus (*in vitro*) in 5 days ([www.translumina.de](http://www.translumina.de)). The EP+PEO surfaces therefore release a lower percentage of the loaded drug than the latter in the same period of time, notwithstanding the fact that the solubility of Sirolimus is two orders of magnitude lower than that of 6-MP (Beuch *et al.* 2007).

The insert of Figure 22 suggests that the acidification of the release medium resulted in a different release rate from EP+PEO samples over the first few hours of immersion (insert of Figure 22). The increase acidification gave rise to a higher rate of release within the first 10 minutes of immersion compared to what had been achieved previously with PBS. It was also seen that the surface of the sample had degraded significantly by the end of the release period when this acidified medium was used (Figure 23).



**FIGURE 23 – SEM IMAGES OF THE SURFACE OF EP+PEO SAMPLES AFTER RELEASE IN (A) HIGHLY ACIDIFIED PBS AND (B) ACIDIFIED PBS**

Further optimization of the release medium is therefore needed in order to ensure drug stability while not damaging the surface and simultaneously giving a more realistic simulation of the stent implantation environment. This can be achieved by using different acids in the optimal concentration or by using another type of simulated body fluid which grants better drug and surface stability while being more relevant to the application environment of these surfaces. Nevertheless, the results obtained show that this medium is a better release medium for visualisation of the sustained release of 6-MP from EP and EP+PEO surfaces under the current drug application conditions.

### 3.3 MATHEMATICAL MODELLING OF DRUG ELUTION

In order to better characterise the release kinetics observed for EP+PEO samples, the data obtained was fitted by means of two models used in literature for the simulation of drug release from polymer-free surfaces: the Korsmeyer-Peppas model (Moseke 2012) and a two-phase elution model based on Ficks' first law of diffusion (Peng 2009).

The Korsmeyer-Peppas model is expressed as:

$$\frac{M(t)}{M_{\infty}} = kt^n \quad \dots (9)$$

where  $M(t)$  is the accumulated released mass at time  $t$ ,  $M_{\infty}$  is the total amount of drug loaded on the surface which would be released at  $t \rightarrow \infty$ ,  $k$  is the kinetic constant and  $n$  is the release exponent (Moseke 2012).

The two-phase Fickian model is expressed as:

$$M(t) = M_{\infty} - M_f \cdot e^{-C_f t} - M_s \cdot e^{-C_s t} \quad \dots (10)$$

where  $M(t)$  is the accumulated released mass at time  $t$ ,  $M_{\infty}$  is the total amount of drug loaded on the surface which would be released at  $t \rightarrow \infty$ ,  $M_s$  is the mass available for slow release,  $M_f$  is the mass available for fast release, and  $C_s$  and  $C_f$  are the first-order kinetic constants for slow and fast release, respectively (Peng 2009).

The use of such a model which does not take into account pore characteristics may be justified by considering the ratio of the radius of the drug molecule to the pore radius. This can be represented as:

$$\lambda = \frac{a}{R_p} \dots (11)$$

When the value of  $\lambda \rightarrow 1$  the steric interaction between the solute molecules and the pore walls is highly influential on the rate of diffusion (Siepmann *et al.* 2012). Diffusing atoms also undergo other forms of interaction with the pore walls such as van der Waals, hydrophobic, dielectric and electrical forces. However, when  $\lambda \gg 1$  all interactions with pore walls become less significant on the bulk rate of diffusion. Moreover, it is known that, under physiological conditions, electrostatic interactions are confined to the area just a few nanometres from the pore wall.

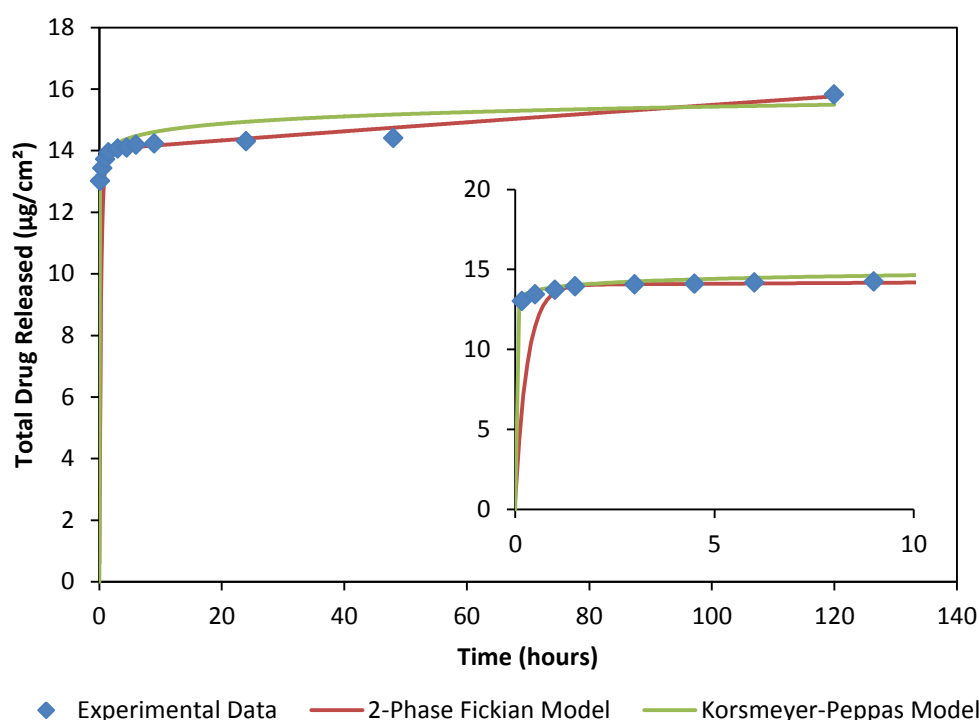
When we consider the porous surfaces investigated in this work, we see that for the EP+PEO surfaces the average pore diameter is in the region of 300nm. When we compare this to the topological diameter of the 6-MP molecule which is 1.65nm (based on the assumption that the shape of the molecule is spherical) we conclude that for EP+PEO surfaces it is not likely to have an influence on the outward diffusion of drug molecules. This justifies the use of first order diffusion based models in order to fit the data obtained experimentally.

The constants required for the two models employed were calculated and tabulated in Table 7.

**TABLE 7 – CONSTANTS USED FOR DRUG RELEASE MODEL DEVELOPMENT**

	Common	Korsmeyer-Peppas		2-Phase Fickian			
Constant	$M_\infty$	$k$	$n$	$M_f$	$M_s$	$C_f$	$C_s$
Value	30.6000	0.4542	0.0227	13.4300	16.5700	3.3214	0.0009

The data for the models of drug release kinetics chosen was therefore generated and plotted with the experimental data in Figure 24. The  $r$  values for the two-phase Fickian and the Korsmeyer-Peppas model data sets compared to the experimental data were 0.99866 and 0.999953 respectively. This shows that both models gave a good fit to the data.



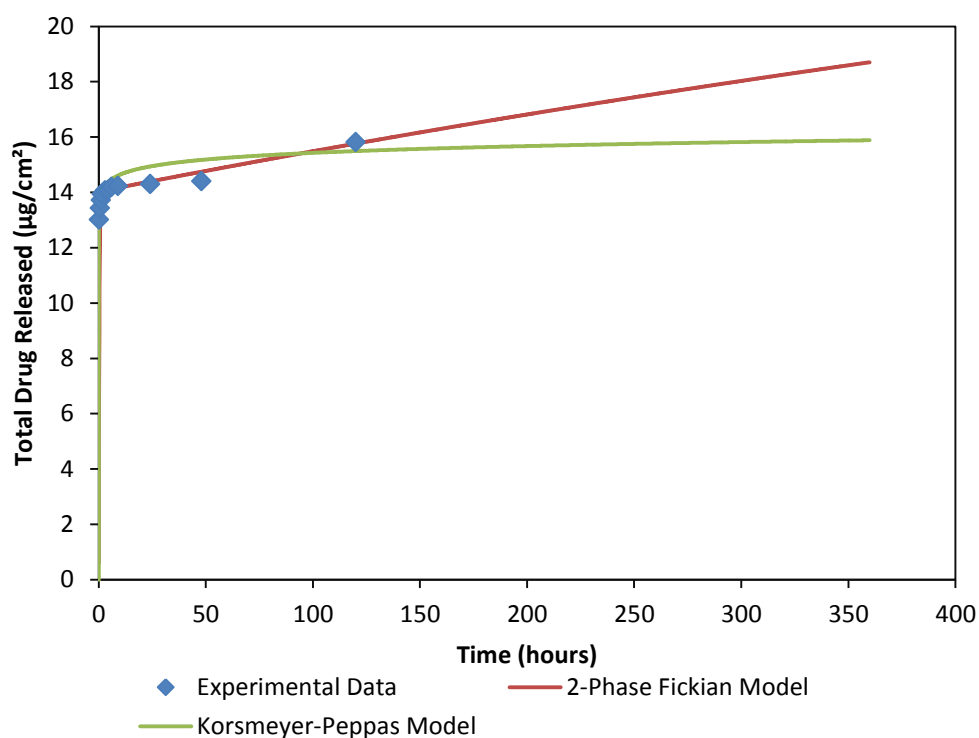
**FIGURE 24 – COMPARISON OF RELEASE KINETICS MODELS TO EXPERIMENTAL 6-MP RELEASE DATA IN PBS + 25mM HCL AT 37°C DURING THE FIRST 120 HOURS OF IMMERSION FROM EP+PEO SAMPLES LOADED BY DRUG SPRAYING 20 LAYERS AT A GAS FLOW RATE OF 192L/HR WITH 30% ETHANOL FINAL RINSING. INSERT SHOWING ENLARGED INITIAL 10 HOUR PORTION.**

The data plotted in however, seems to suggest that the 2-Phase Fickian model gives a better fit when we consider the first 120 hours of release. The  $r$  values obtained can be understood by looking at the first 10 hours of release. In the latter it can be seen that for the first two data points there is a very large difference between the values measured experimentally and those predicted by the Fickian model. On the other hand, it can also be seen that during the initial phases of release the Korsmeyer-Peppas model gives a very good fit. However, since the main aim of the PEO treated Nitinol used in this project is to provide a sustained release of the drug over a long period of time, the model chosen to describe the release must be valid over longer periods of time than the ones currently investigated.

Although both models gave a good fit, the data plotted in Figure 24 seems to suggest that the 2-Phase Fickian model gives a better fit to the two-phase release measured experimentally. A closer look at the fitting curves (insert Figure 24) indicates that during the initial phases of release (burst) the Korsmeyer-Peppas model gives a very good fit. However, since the main aim of the PEO treated Nitinol is to provide a sustained release of the drug over longer periods of time, the model was extrapolated to 360 hours (Figure 25). Here it becomes evident that the Korsmeyer-Peppas model does not describe the release kinetics adequately since it is known that the average



total load of 6-MP is  $30.6\mu\text{g}/\text{cm}^2$  and the release predicted by this model seems to flatten out. Future work should therefore extend the experimental release period further in order to be able to assess whether the two-phase Fickian model gives an adequate approximation of the release kinetics involved.



**FIGURE 25 – MODEL EXTRAPOLATION TO 360 HOURS OF RELEASE IN COMPARISON TO EXPERIMENTAL DATA FOR FIRST 120 HOURS OF RELEASE.**

The properties of the drug itself influence the diffusion from porous structures. Since our system consists of a drug which is deposited onto the surface and is allowed to crystallise within the porosity, the drug molecules must first dissolve from the crystallised solid and then diffuse out of the porous surface layer. The rate of diffusion out of the surface is therefore governed by the solubility of the drug within the release medium. This factor puts the system chosen for this project at a clear disadvantage since the solubility of 6-MP in water is two orders of magnitude higher than the solubility of Sirolimus, which is the gold-standard anti-restenotic drug. Loading the EP+PEO surfaces with drugs like Sirolimus under the same loading conditions would therefore be useful in order to assess their potential for sustained release. Furthermore, it would enable the direct comparison of the release profiles obtained with those available for the Yukon stents. Investigation with other drugs, such as indomethacin, would permit the comparison of the release kinetics with the data published for polymer-free drug elution from  $\text{TiO}_2$  nanotubes by Aw *et al.* (2011 & 2012), Gulati *et al.* (2012) and Losic *et al.* (2011).



## 4. CONCLUSIONS

---



## 4 CONCLUSIONS

This project dealt with the assessment of the potential of PEO treated NiTi surfaces to sustain the release of the novel anti-restenotic drug 6-MP.

A microporous titania layer was created on the surface of Nitinol samples by means of electropolishing followed by plasma electrolytic oxidation. The surfaces produced were found to have a wide range of pore diameters varying from a couple of microns to a couple of tenths of a micron, with an average pore diameter of  $0.356\mu\text{m}$  and a surface porosity of approximately 10%. Furthermore, it was seen that this treatment gave rise to a decrease in the water contact angle from  $28.7^\circ$  in the electropolished samples to  $11.2^\circ$  but caused no significant changes in the surface roughness.

EP and EP+PEO treated surfaces were loaded with 6-MP by spraying 20 layers of an aqueous solution of the drug with intermediate drying and a final rinsing step in 30% ethanol. An average of  $18.2\text{ }\mu\text{g}/\text{cm}^2$  and  $30.6\text{ }\mu\text{g}/\text{cm}^2$  of 6-MP was loaded on the EP and EP+PEO samples, with a drug loading efficiency of 26.8% and 41.9%, respectively. The release of the drug in PBS at  $37^\circ\text{C}$  for EP+PEO samples showed a burst of 37% of the loaded drug, followed by a more gradual release in the first 6 hours. Comparatively, EP surfaces showed only a high burst (78%) in the first 10 minutes of immersion. In both cases, however, a high rate of drug degradation was observed at longer durations.

The stability of 6-MP in various media was studied in order to understand which factors were influencing the degradation during the release experiments. Results indicated that PBS gave rise to a degradation of approximately 50% within 10 days while only 1.5% degradation was seen in highly acidified PBS during the same period of time.

The release of 6-MP from EP+PEO surfaces in acidified PBS solution showed two-phase release kinetics: a burst phase where 42% of the drug was released, followed by a slow sustained release of the drug over the following 5 days of immersion. By the end of the release period studied, EP+PEO surfaces had released 52% of the loaded drug. On the other hand, EP surfaces showed a release of 95% of the loaded drug within the first 10 minutes of immersion.

The experimental data collected for EP+PEO samples was compared to two models of drug release kinetics based on diffusion; namely, a two-phase Fickian diffusion model and the Korsmeyer-Peppas model. Although both models showed a good fit,

the extrapolation of the data to extended times suggested that the two-phase Fickian diffusion model gave results which were closer to the ones expected. Further validation of this model must however be conducted by extending the experimental release period.

This study has shown that EP+PEO surfaces are effective at sustaining the release of 6-MP over a period of 5 days when loaded by spraying 20 layers of an aqueous solution of the drug. The results indicate that Nitinol surfaces modified by PEO may be used as polymer-free drug carriers for biomedical applications.

## 5. SUGGESTIONS FOR FUTURE WORK

---





## 5 SUGGESTIONS FOR FUTURE WORK

This study was the first of its kind in the drug employed, in the chemistry of solvent used for the drug, in the drug application method for a fully-polymer-free system and in the surface modification which was applied to the Nitinol samples. This means that a lot of the work done was highly exploratory leading to the identification of a large number of areas which need to be investigated further in future work.

Firstly, it is necessary to expand the research on the issues related to drug stability. It is clear that using highly acidified PBS as the release medium is not ideal from a bio-medical perspective. This medium can in no way be considered to simulate the environment present at the stent-arterial wall interface upon stent deployment and was only chosen as a release medium since, from the media investigated, it was the most effective at halting drug degradation. A new release medium which is more representative of the implantation environment but which simultaneously enables drug stability must therefore be formulated.

Moreover, since the issues with drug stability were found to be partly due to the solvent employed in the 6-MP solution which was used for spraying, future work must also find better solvents for the drug. Alternative spraying systems might be sought in order to allow the use of organic solvents since no mention of drug instability in such solvents was found in the literature reviewed on the drug. However, chemical modifications of the drug, such as methylation, have to be taken into consideration in the selection of the solvent. Careful selection of organic solvents would also allow for higher drug concentrations in the stock solutions, therefore enabling the application of higher drug loads within a feasible number of sprayed layers.

Another area which deserves further attention is the method of drug application. In this study the main focus was spraying and only a few variants were put forward to the release experiments. Further experimentation with the gas flow rate, the drug solution flow rate, the number of sprayed layers and the length of each spraying cycle must be conducted in order to find the ideal drug application method. New experiments might also consider the use of intermediate washing steps since this study revealed that the inclusion of a washing step at the end of drug loading resulted in a more uniform distribution of the drug on the surfaces investigated.

In order to be able to compare the results obtained with those published by other researchers in the area, it would also be ideal to perform the same drug loading procedures using the standard drugs used in literature. Furthermore, it may be of inter-

est to investigate the role of drug solubility and molecular size on the release kinetics.

In order to better quantify the release potential of the porous drug carrier, thermal gravimetric analysis should be used to determine the amount of drug loaded on the samples and that which is still present on the surface at the end of the release period. The latter would enable a more precise calculation of the percentage of drug released at each time point. This was not possible in this work since the only analysis equipment available was HPLC and would therefore require the drug still present on the surface to be brought into solution and the lowest drug concentration which could be measured using this equipment was in the region of 100ng/ml.

## 6. LIST OF REFERENCES

---



## 6 LIST OF REFERENCES

Abazaid, A., Costa, R., 2010. New Drug-Eluting Stents: An Overview on Biodegradable and Polymer-Free Next-Generation Stent Systems. *Circulation: Cardiovascular Interventions*, 3, pp. 384-393.

Aw, M.S., Simovic, S., Addai-Mensah, J., Losic, D., 2011, Polymeric micelles in porous and nanotubular implants as a new system for extended delivery of poorly soluble drugs. *Journal of Materials Chemistry*, 21, pp. 7082-7089

Aw, M.S., Addai-Mensah, J., Losic, D., 2011. Polymeric micelles for delayed release of therapeutics from drug releasing surfaces with nanotubular structures. *Macromolecular Bioscience*, 12, pp. 1048-1052.

Byrne, R.A., Mehilli, J., Iijima, R., Schulz, S., Pache, J., Seyfarth, M., Schömig, A., Kasrati, A., 2009. A polymer-free dual drug-eluting stent in patients with coronary artery disease: a randomized trial vs. polymer-based drug-eluting stents. *European Heart Journal*, 30, pp. 923-931.

Buech, G., Bertelmann, E., Pleyer, U., Siebenbrodt, I., Borchert, H.H., 2007. Formulation of Sirolimus eye drops and corneal permeation studies. *Journal of Ocular Pharmacology and Therapeutics*, 23(3), pp.292-303

Curran, J.A. and Clyne, T.W., 2006. Porosity in plasma electrolytic oxide coatings. *Acta Materialia*, 54, pp. 1985-1996.

Dong, H., 2010. *Surface Engineering of Light Alloys – Aluminium, magnesium and titanium alloys*, Woodhead Publishing Limited, CRC Press.

Garg, S. and Serruys, P.W., 2010. Coronary stents – Looking forward. *Journal of the American College of Cardiology*, 56(10), pp. S43-S78.

Gulati, K., Ramakrishnan, S., Aw, M.S., Atkins, G.J., Findlay, D.M., Losic, D., 2012. Biocompatible polymer coating of titania nanotube arrays for improved drug elution and osteoblast adhesion. *Acta Biomaterialia*, 8, pp. 449-456.

Gultepe, E., Nagesha, D., Sridhar, S., Amiji, M., 2010. Nanoporous inorganic coatings for sustained drug delivery in implantable devices. *Advanced Drug Delivery Reviews*, 62, pp. 305-315.

Huan, Z., Fratila-Apachitei, L.E., Apachitei, I., Duszczek, J., 2012. Porous NiTi surfaces for biomedical applications. *Applied Surface Science*, 258, pp. 5244-5249.

Khan, M.G., 2011. *Encyclopedia of Heart Disease*. 2<sup>nd</sup> Ed. Humana Press, Springer

## Reference.

Kröplin, T., Weyer, N., Gutsche, S., Iven, H., 1998. Thiopurine S-methyltransferase activity in human erythrocytes: a new HPLC method using 6-thioguanine as substrate. *European Journal of Clinical Pharmacology*, 54(3), pp. 265-271.

Kukreja, N., Onuma, Y., Daemen, J., Serruys, P.W., 2008. The future of drug eluting stents. *Pharmacological Research*, 57, pp.171-180.

Kutz, Myer (ed)., 2009. *Biomedical Engineering and Design Handbook, Applications*, Volume 2, 2<sup>nd</sup> Ed., Mc Graw Hill Publishers

Losic, D., Velleman, L., Kant, K., Kumeria, T., Gulati, K., Shapter, J.G., Beattie, D.A., Simovic, S., 2011. Self-ordering electrochemistry: A simple approach for engineering nanopore and nanotube arrays for emerging applications. *Australian Journal of Chemistry*, 64, pp. 294–301.

Marieb E.N., Hoehn, K., 2010. *Human anatomy and Physiology*, 8<sup>th</sup> edition, Pearson international edition, pp. 694-751.

Massberg, S., Byrne, R.A., Kastrati, A., Schulz, S., Pache, J., Haysleiter, J., Ibrahim, T., Fusaro, M., Ott, I., Schömig, A., Laugwitz, K.L., Mehilli, J., 2011. Polymer-free Sirolimus- and Probucol-eluting versus new generation Zotarolimus-eluting stents in coronary artery disease. The intracoronary stenting and angiographic results: Test efficacy of Sirolimus- and Probucol-eluting versus Zotarolimus-eluting stents (Isar-Test 5) Trial. *Circulation*, 124, pp. 624-632.

Moseke, C., Hage, F., Vorndran, E., Gbureck, U., 2012. TiO<sub>2</sub> nanotube arrays deposited on Ti substrate by anodic oxidation and their potential as a long-term drug delivery system for antimicrobial agents. *Applied Surface Science*, 258, pp. 5399-5404.

Peng, L., Mendelsohn, A.D., LaTempa, T.J., Yoriya, S., Grimes, C.A., Desai, T.A., 2009. Long term small molecule and protein elution from TiO<sub>2</sub> nanotubes. *Nano Letters*, 9(5), pp.1932-1936.

Pires, N.M.M., Pols, T.W.H., de Vries, M.R., van Tiel, C.M., Bonta, P.I., Vos, M., Arkenbout, E.K., Pannekoek, H., Jukema, J.W., Quax, P.H.A., de Vries, C.J.M., 2007. Activation of Nuclear Receptor Nur77 by 6-Mercaptopurine Protects Against Neointima Formation. *Circulation*, 115, pp. 493-500.

Pols, T.W.H., Bonta, P.I., Pires, N.M., Otermin, I., Vos, M., de Vries, M.R., van Eijk, M., Roelofsen, J., Havekes, L.M., Quax, P.H., van Kuilenburg, A.B.P., de Waard, V., Pannekoek, H., de Vries, C.J.M., 2010. 6-Mercaptopurine Inhibits Atherosclerosis in Apolipoprotein E\*3-Leiden Transgenic Mice Through Atheroprotective Actions on Monocytes and Macrophages. *Arteriosclerosis, Thrombosis and Vascular Biology*, 30, pp.1591-1597.

Puskas, J.E., Muñoz-Robledo, L.G., Hoerr, R.A., Foley, J., Schmidt, S.P., Evancho-Chapman, M., Dong, J., Frethem, C. Haugstad, G., 2009. Drug-eluting stent coatings. *WIREs Nanomedicine and Nanobiotechnology*, 1, pp. 452-462.

Shabalovskaya, S., Anderegg, J., van Humbeeck, J., 2008. Critical overview of Nitinol surfaces and their modifications for medical applications. *Acta Biomaterialia*, 4, pp.446-467.

Siepmann, J. *et al.*, *Fundamentals and Applications of Controlled Release Drug Delivery*, Advances in Delivery Science and Technology. Controlled Release Society, 2012.

Thierry, B., Merhi, Y., Bilodeau, L., Trépanier, C., Tabrizian, M., 2002. Nitinol versus stainless steel stents: acute thrombogenicity study in an ex vivo porcine model. *Biomaterials*, 23, pp. 2997-3005.

Venkatraman, S., Boey, F., 2007. Release profiles in drug eluting stents: Issues and uncertainties. *Journal of Controlled Release*, 120, pp.149-160.

Waranis, R.P., Siver, K.G., Sloan, K.B., 1987. The solubility parameter of vehicles as a predictor of relative vehicle effects on the diffusion of 6-mercaptopurine. *International Journal of Pharmaceutics*, 36, pp. 211-222.

Wessely, R., 2010. New drug-eluting stent concepts. *Nature Reviews. Cardiology*, 7, pp.194-203.

Yoneyama T., Miyazaki, S., 2009. *Shape memory alloys for biomedical applications*, Woodhead Publishing Limited, CRC Press.